Journal of Applied Polymer Science

WILEY

Applied Polymer SCIENCE

RESEARCH ARTICLE OPEN ACCESS

Relationships Between Mechanical Behavior and Structure/Properties for Macroscopically Homogeneous Porous Composites Containing Randomly Shaped Filler

Miroslav Černý[1] | Přemysl Menčík[1,2]

[1]Faculty of Chemistry, Brno University of Technology, Brno, Czech Republic | [2]Central European Institute of Technology, Brno University of Technology, Brno, Czech Republic

Correspondence: Miroslav Černý (miro.ce@centrum.cz)

Received: 10 August 2023 | **Revised:** 31 October 2024 | **Accepted:** 14 November 2024

Funding: This work was supported by the Brno University of Technology [Specific University Research Grant FCH-S-23-8208].

Keywords: composites | mechanical properties | porous materials

ABSTRACT

The work focuses on researching relationships between structure/properties and mechanical behavior of porous composites. The primary data comes from tensile testing. The observed properties include elastic modulus, ultimate strength, ultimate strain, and energy need for ultimate strength achievement. The studied materials include composites based on different polyurethane matrices and one rubber filler with various filler and porosity contents. Presented work expands the possibilities of an approach based on measured data fitting by a suitable function followed by obtained parameters interpolation. The utilization of new structural parameters leads to a spatial linear function shape instead of spatial exponential. The newly introduced equation is $z_c = z_m + z_m \cdot (b \cdot p_1 + c \cdot p_2)$, where z_c/z_m is generally labeled mechanical property value for composite/nonporous matrix, p_1/p_2 are suitable structural parameters, and b/c are fitting parameters subjected to interpolations by logarithmic function containing values of properties typical for matrices. The work focuses on studying the case of different matrices and one kind of filler. The work includes all potentially valuable interpolations for earlier mentioned properties with the most interesting results in cases of pairs p_1/p_2 containing two from three parameters: n (porosity), $1-v_m$ (v_f + porosity), and v_f (filler volume fraction).

1 | Introduction

Understanding the behavior of materials around us (including those porous) is important. The ability to predict material behavior can be the decisive parameter to its successful utilization. Materials can differ in their complexity in composition and structure. Except for the matrix, they can include fillers, reinforcement, and porosity. The term structure can also contain the shape of particles and voids, which can affect how the material will behave under loading. Description of the material behavior is usually more difficult as the material is more complex in composition and structure. This interested materials containing (except matrix) particles, voids, and mainly both of them.

First, it is necessary to mention the one-component porous materials. Many authors have endeavored to find some relationships between structure/composition and chosen mechanical properties. But the works were usually dedicated only to one material type with different degrees of porosity as porous metal [1–5], ceramics [1, 4, 6–14], polymers [1, 15], and natural materials [16]. The describing functions acquire different mathematical forms. The mathematical types of dependencies usually using some adjustable fitting parameter(s) are linear [1, 5–7, 9–13], exponential [1, 5, 6, 11, 12], power [1–4, 6, 9, 11, 12, 14, 15, 17–19], and logarithmic [5].

The more difficult situation is in the description dedicated to the more complex materials—composites. There are two

approaches for describing or predicting the material behavior, which can be illustrated in the porous composites [20]. The first approach means different models [21–26] and simulations using various mathematical methods such as Fast Fourier Transform [27], finite element method [28, 29], or fractals [21]. These solutions depend on the exact physical knowledge and simplifying expectations about the composition and structure of the microscopic levels in studied materials. These expectations can vary a lot according to chosen research work. The expected limits can mean shapes of filler as granular particles [30], short fibers with cylindrical shapes [28], or circular cross-sections [27]. Forms of voids can be limited to spherical [25]. Expectations can include the exclusion of contact among pores and (short) fibers [28] or particles [21] or even the separation of one bulk phase and the open porosity by the surface phase [29]. Pores and filler are expected nano-sized in both cases [27] or only particles in the form of nanotubes or nanoparticles [23, 24]. Specific requests include the unidirectional orientation of nanofibers [27] and splitting the filler according to size distribution and location of different fractions in different domains [21]. The approach using various models and simulations predominates in the literature. It is used for the research of elastic region of loading [21, 26–28] and also for the nonlinear stress [22–24, 29, 30] with the comparisons between expected results and measured results from a provided measurement on materials.

The second approach observes the material from a macroscopic point of view concerning the properties of its components. The first part is the measurement when the measured data can be subjected to fitting by a suitable function with the following interpolation of obtained parameters to reach dependence between properties and structure/composition of the material. Work dedicated to tensile testing of porous composites containing nanofibers and describing their fracture probability according to fracture toughness and porosity by Weibull analysis [31] is an example of a macroscopic point of view.

The presented article directly follows previous work based on porous composite materials containing various polyurethane matrices with the connection of rubber filler [32, 33]. The measured data from tensile loading were subjected to fitting by spatial exponential functions represented by Equations (1 and 2) [32] and respectively (3) [33].

$$z_c = z_m \cdot v_m^b \cdot \left(1 - v_f\right)^c \tag{1}$$

$$z_c = z_m \cdot v_m^b \cdot n_p^c \tag{2}$$

$$z_c = z_m \cdot n_p^b \cdot \left(1 - v_f\right)^c \tag{3}$$

where z_c and z_m are general labels for properties represented by elastic modulus (E), ultimate strength and strain (σ_{Fmax} and ε_{Fmax}), and energy need for ultimate strength achievement (A_{Fmax}). The functions include also structural parameters v_m, $1 - v_f$, and n_p (matrix volume fraction, interspace volume—volume fraction of space among filler particles in the material, ad interspace filling—how much the matrix fulfills the interspace volume). The previous paper [32] also mentioned two other structural parameters—$1 - n$ (solid rate of material) and n_{pf} (matrix rate in the solid rate of material = matrix volume fraction in case of porosity neglect). These parameters are dimensionless and can have a range of values from 0 to 1. The exponents b and c are parameters ensuring the best mathematical fitting. The structural parameters are coupled into pairs because each pair is composed of two structural parameters that can describe the composition of material containing matrix, voids, and filler only together. Therefore there are three equations, including Equations (1–3), where multiplication is used between the basic members because the structural parameters v_m, $1 - v_f$, and n_p are equal to 1 for nonporous matrix and equal to 1 or lower for more complex material. The b and c parameters have the form of exponents to be distinguished for different structural parameters.

The b and c parameters have been then subjected to interpolation. The example is Equation (3) depicting interpolations in the case of elastic modulus in Equation (4):

$$E_c = E_m \cdot n_p^{d+e\cdot\ln E_m} \cdot \left(1 - v_f\right)^{f+g\cdot\ln\left(E_m\cdot\delta\right)} \tag{4}$$

where E_c and E_m are elastic modulus values for the composite and the nonporous matrix. δ is the OH/NCO ratio before the curing of the polyurethane matrix. δ served as an assumption of matrix polarity related to adhesion to filler (rubber in all cases). Parameters d, e, f, and g should reflect the relations between filler and matrix, but these relations were assumed only due to the utilization of only one type of filler—rubber. Therefore, previous works did not solve these relations [32, 33]. The assumption of d, e, f, and g connection to the description of filler properties or its relation to the matrix came from the idea that the parameters d, e, f, and g were the last remaining members without clear description in suggested equations and the last not described phenomenon was the description of the filler function in the composite including filler relations to the matrix. It is suitable to mention that this phenomenon consideration is quite important because it should also include a filler influence of porosity, which can be affected by filler presence, concentration, and its type in the material.

The Equations (1–3) can be simplified to obtain relationships for less complex materials. An example of the porous matrix is Equation (5):

$$z_{mn} = z_m \cdot (1 - n)^b \tag{5}$$

where z_{mn} means property value for porous matrix, and n is dimensionless porosity (can acquire values from 0 to 1). Equation (5) occurred under different labeling and also in other sources dedicated to different mechanical properties such as elastic modulus [10, 34] and strength [1, 35]. The exponent b was presented in the mentioned works [1, 10, 34, 35] as a constant with values differing according to material type. The member $1 - n$ in Equation (5) is equal to n_p in the case of a porous matrix, respectively v_m (while $1 - v_f = 1$).

To show the porous composites as recently studied topics, papers dedicated to porous composites differing by their compositions and potential applications instead of a general description of the connection between the structure and properties can be mentioned. The examples include regenerated cellulose/cross-linked

poly(ethylene glycol) reaching up to 97% porosity for potential biomedical applications, packaging and sewage purification [36], properties of glass–ceramic/nanocopper [37], alloy composed of titanium, aluminum and vanadium/silver particles reaching up to 50% of porosity for biomedical applications [38], and even ceramics/epoxy resin or polycaprolactone with approximately 70% of porosity [39].

The main goal of this article is to contribute to a description of relationships between structure/composition and properties for porous-filled composites. It directly follows earlier works [32, 33] and uses the same primary data set. It should effort another insight by using complementary structural parameters to those (n_p, v_m, $1-v_f$, etc.) used in previous articles [32, 33], because the complementary parameters introduced in this paper embody different mathematical behavior. They could then lead to new contributions in describing the behavior of porous materials. The mechanical behavior dependencies of porous composite materials are not fully known, and each contribution could stand significant.

2 | Materials and Methods

2.1 | Materials

This work uses the same primary dataset as previous works [32, 33], as mentioned in the introduction. The original data come from tensile testing of porous composites and the corresponding porous matrices (nonporous matrices and composites were unavailable due to the porous nature of used polyurethane matrices). All 10 used matrices were based on the same MDI (methylene-di-phenyl-di-isocyanate) pre-polymer Unixin 4223CS (Lear, Czech Republic, 6.9 wt% of isocyanate (NCO) groups, number average of molecular weight 690 g/mol, viscosity 2800 ± 500 mPa s), used the same accelerator (Lear, Czech Republic, di-butyl-tin-di-laureate, DBTL) and differed by used curing agents including castor oil (Fichema, Czech Republic), distilled water and glycerol (Penta Chemicals, Czech Republic). Some of the matrices included suitable modifying components such as linseed oil serving as a plasticizer (Fichema, Czech Republic) or inorganic fillers in powder forms of quartz (Millisil W12, Provodínské Písky, Czech Republic), calcite and iron (both of them from Pkchemie, Czech Republic, 14–16 wt% of silicon in iron) serving for the matrix stiffening to reach higher diversity in observed mechanical properties range of matrices without changes of rate or kind of curing agent. The composition of matrices in vol% is in Table 1 with the OH/NCO rate in polyurethane before curing labeled δ and designation used throughout the entire article. Particle size distributions of quartz, calcite, and iron are in Figure S1.

The composite materials contained except matrix also rubber filler. The rubber filler was supplied and used in three fractions labeled R_0–R_2 (RGP Recycling, Czech Republic, higher index number means larger particles). The knife milling served for R_1 and R_2 fractions manufacturing. The milling with a rolling machine led to R_0 manufacturing. The origin of rubber filler was the same in all cases—waste car tires. The size distributions of R_0 and R_1 rubber (and also of inorganic fillers) are in Figure 1 and come from laser analysis (HELOS (H2568) & RODOS). The laser analysis was not appropriate for R_2 distribution due to the large dimensions of particles, and it was obtained only partially by the sieve analysis. The particle shapes of all fillers are in Figure S2 and come from scanning electron microscopy (TESCAN MIRA 3 for inorganic fillers and Carl Zeiss EVO LS 10 for rubber). The densities of all fillers were measured by a pycnometer three times. The average values are 1.18 g/cm^3 for

TABLE 1 | Chemical composition of PUR samples serving as matrices for composites.

Designation	PU4223 CS (vol%)	Curing agent (vol%)	Others (vol%)	δ[a] (–)	ρ_t (g cm^{-3})	n_m (%)
P_{99}-W_1	99	1 (W)	—	0.68[b]	1.10[c]	57 ± 7
						16 ± 2
P_{95}-G_5	95	5 (G)	—	1.22	1.12[d]	9.5 ± 0.7
P_{80}-G_{20}	80	20 (G)	—	5.79	1.15[d]	10 ± 1
P_{85}-G_5-CO_{10}	85	5 (G) +10 (CO)	—	1.55	1.05[d]	2 ± 2
P_{65}-CO_{35}	65	35 (CO)	—	0.87	1.04[d]	4 ± 1
P_{49}-CO_{26}-LO_{25}	49	26 (CO)	25 (LO)	0.87	1.03[d]	1 ± 2
P_{33}-CO_{17}-Si_{50}	33	17 (CO)	50 (Si)	0.87	1.85[e]	16 ± 1
P_{33}-CO_{17}-Ca_{50}	33	17 (CO)	50 (Ca)	0.87	1.86[e]	32 ± 2
P_{33}-CO_{17}-Fe_{50}	33	17 (CO)	50 (Fe)	0.87	4.04[e]	22.6 ± 0.5
P_{72}-G_{18}-Ca_{10}	72	18 (G)	10 (Ca)	5.79	1.30[e]	16.3 ± 0.6

Note: Pre-polymer: PU4223 CS (P); curing agents: Water (W), glycerol (G), castor oil (CO); plasticizer: Linseed oil (LO); fillers included in matrices: SiO_2 (Si), $CaCO_3$ (Ca), Fe (Fe) [32]. Reference [33] is Reprinted by permission from Springer Nature Customer Service Centre GmbH: Springer Nature, SN Applied Sciences.
[a]Reflecting OH/NCO molar ratio.
[b]For this purpose, H_2O represents two OH groups.
[c]Measured by pycnometer method.
[d]Obtained from knowledge about volume, mass, and porosity.
[e]Calculated via simple mixing equation.

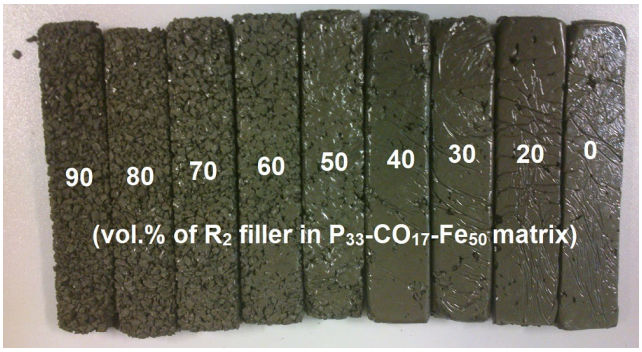

FIGURE 1 | Example of different filler content on samples based on one pair matrix/filler. The value of volume percentage is valid in case of porosity neglect. [Color figure can be viewed at wileyonlinelibrary.com]

all rubber fractions, 2.65 g/cm^3 for quartz, 2.68 g/cm^3 for limestone, and 7.03 g/cm^3 for iron.

2.2 | Preparation and Testing of Samples

The preparation of samples was manual. First, liquid components were mixed (pre-polymer, curing agent(s), accelerator, and plasticizer, if it was a part of the matrix). The addition of the rubber (only one fraction in all cases) or its mixture with inorganic filler to the liquid part followed. The curing of the final blend was carried out under ambient conditions. The stainless steel molds were equipped with low-density polyethylene foil for better separation and used for the curing.

Each used filler/matrix combination underwent the density and porosity measurement. Fillers and the P_{99}-W_1 matrix (matrix labeling is in Table 1, measuring only thoroughly chosen pieces having no pores) underwent the pycnometer method (using the average from three results). The other matrices without inorganic rate were subjected to direct measurement of volume (in ethanol) and weight (8–18 g, by analytical balance) to obtain the density of porous matrices (used average from three measurements). The measurement continued with porosity observation by a confocal microscope (in optical mode). Ten figures of each matrix were obtained from the fracture surface area to get the rate of pores from each figure. The porosity and density averages gave the hypothetical nonporous matrix density value used in further calculations. The measurement of composite samples (beams) was based on measurements of dimensions (by digital caliper) and weighting. The knowledge about the theoretical (= nonporous) composition, density of partial components, and the measured density value led to the value of porosity of each composite sample according to the equation:

$$n = 1 - \frac{\rho}{\rho_t} = 1 - \frac{\frac{m}{V}}{\Sigma v_{it} \cdot \rho_{it}} \quad (6)$$

where n is porosity, ρ is measured density, ρ_t is theoretical density, m is weight, and V is the sample volume. The labels v_{it}, and ρ_{it} represent the volume fraction and the density of the ith component of the composite. The porosity of composites could not be accurately controlled and was measured after sample preparation. The porosity values were variable according to the filling extent and could be close to 50% of material volume and even exceed it in rare cases [32].

The beam dimensions for tensile testing were 120 mm × 24 mm × 12 mm and their values were a compromise ensuring the suppression of porosity effect to the stability of observed properties values and also adequate saving of input material due to a lot of samples (beams) including not only matrices but mainly composites based on them. Cross-head speed was 30 mm s^{-1}. Elastic modulus came from the strain range of 0.05%–0.25%. Testing machine was ZWICK Z010 ROELL. The output included values of elastic modulus (E), ultimate strength (σ_{Fmax}), ultimate strain (ε_{Fmax}), and energy need for ultimate strength achievement (A_{Fmax}) calculated by the following equation:

$$A_{\mathrm{Fmax}} = \sum \left(\varepsilon_n - \varepsilon_{n-1}\right) \cdot \frac{\sigma_n + \sigma_{n-1}}{2};\ n \in \langle 1; n_{\mathrm{Fmax}} \rangle \quad (7)$$

where symbols σ_n, σ_{n-1}, ε_n, and ε_{n-1} are the strength and strain values of neighboring points on the tensile curve. n_{Fmax} represents the maximum force point. Joule per cubic meter is the basic unit of A_{Fmax} [32, 33]. The values of properties belonging to the yield point were not present due to the missing yield point of samples.

The range of filling with rubber was 20–90 vol% with a 10% increment for all matrices. Values are valid in case of porosity neglect. This concentration set was used independently for all three rubber fractions except for the high filling of mainly lower filler fractions with combinations of some matrices. The detailed scheme of prepared and tested samples is in Figure S5. The beams creating examples with different filler contents are in Figure 1. Figure 1 also indicates the porosity rate, which usually decreases with increasing filler volume fraction. The solid filler then replaces the porous matrix. When the filler content exceeds some value differing according to matrix porosity, the matrix cannot fulfill the space between filler particles, and the porosity increases. It is usually the highest when the filler content is also highest and reaches up to 50 vol% of closed and open pores together.

2.3 | Base of Calculations

Plenty of symbols are in this work. The explanations of labels are in Table S1. Table S2 contains the significance, meaning, and source for chosen parameters if they are significant for calculations. The Supporting Information section contains some schemes for a better understanding of the basic principles of this work. The scheme generally shows the data processing from the measurement to the final equations in Figure S1. Figure S2 contains the scheme of the work from rough materials through a system of prepared samples to obtain data.

This work varies in structural parameters from those used or mentioned by previous works (n_p, v_m, $1-v_f$, $1-n$, and n_{pf}) [32, 33]. Although this work uses the same method to transform the composition and structure from a macroscopic point of view into relationships describing mechanical properties,

it leads to different equations without collisions to those published earlier—Equations (1–3). The calculation method contains two steps too. The first is fitting ensured by the least squares method repeated many times. It leads to values of b and c parameters and the z_m value. The second step is an interpolation of b and c parameters by z_m and other utilizable properties of matrices in some cases. The integral area under the matrix tensile curve described by Equation (8) acquires values between 0 and 1 is significant for ultimate strength. The $\sigma_{m,Fmax}$, $\varepsilon_{m,Fmax}$, and $A_{m,Fmax}$ come from tables as values for nonporous matrices—Tables 4–6. δ (OH/NCO rate in the matrix before curing) is significant for elastic modulus and ultimate strength. The resulting general equation shape and description of members meaning are in Section 2.3. The basic form of equations connecting the structure/properties with behavior is the main result of this work.

$$S_{m,rel} = \frac{A_{m,\mathrm{Fmax}}}{\sigma_{m,\mathrm{Fmax}} \cdot \varepsilon_{m,\mathrm{Fmax}}} \tag{8}$$

The previous works [32, 33] include structural parameters equal to 1 when the matrix does not contain pores and particles. However, there is also a definition possibility of complementary structural parameters to v_m, $1-v_f$, n_p, n_{pf}, and $1-n$. It implies the question about their possible utilization in describing the behavior of porous composites. An example of such parameter calculation is in Equation (9):

$$n_n = 1 - n_p \tag{9}$$

where n_n is interspace porosity (porosity rate in the interspace = space among filler particles respectively the whole volume of the sample for unfilled samples). Analogically to Equation (9) there are defined the remaining parameters v_f (filler volume fraction) from $1-v_f$; $1-v_m$ (volume fraction of filler and porosity) from v_m; n (porosity) from $1-n$; and n_{fp} (filler rate in the solid rate of material = filler volume fraction in case of porosity neglect) from n_{pf}. All complementary structural parameters can be subsequently derived in the direction from n calculated by earlier mentioned Equation (6) to n_{fp} with knowledge of sample values of v_{mt} (volume fraction of matrix, in case of porosity neglect) as it is in the following equations:

$$n_n = \frac{n}{n + \frac{v_{m(t)}}{1 + \frac{n}{1-n}}} \tag{10}$$

$$v_f = 1 - n \cdot \left(1 + \frac{1-n_n}{n_n}\right) = (1-n) \cdot \left(1 - v_{mt}\right) \tag{11}$$

$$1 - v_m = v_f + n \tag{12}$$

$$n_{fp} = \frac{v_f}{1 - \left(1 - v_m\right) + v_f} = \frac{v_f}{v_f + v_m} \tag{13}$$

The complementary structural parameters are generally equal to 0 in the case of the nonporous matrix. Some of these parameters are equal to 0 in the case of nonporous composite (n, n_n) and porous matrix (n_{fp}, v_f). It means that the general multiplication between structural parameters, as occurs in Equations (1–3) mentioned in the introduction and coming from works [32, 33], cannot be used. Addition or subtraction has to replace the multiplication of structural parameters. This sign change ensures a positive non-zero value of the pair of parameters when one parameter equals 0 and the second is non-zero. It needs a relationship change between structural parameters and matrix property that creates a slope in Equation (1–3). The matrix property value should not be only the slope but also displacement in linear function, or only displacement when the slope value equals one and serves as the slope after reproaching. Splitting the matrix property to slope and displacement ensures a direct connection between matrix property and structural parameters and necessary partial separation, for example, in the case of a nonporous matrix when both structural parameters equal 0. The fitting parameter(s) need not be a power but, for example, a multiplier. This idea returns to the Equation (5). It is a simplification of Equations (1–3), where is structural parameter $1-n$ valid only for porous matrices united from the n_p and v_m typical for more complex systems. When the $1-n$ parameter is part of an analogous equation to Equation (9), it leads to n—porosity. Equation (9) could then connect not only the different structural parameters from Equations (1–3) but also different approaches of either n_p, v_m, and $1-v_f$ parameters or their complementary counterparts. Although, there is no clear mathematical role of the b parameter transformation because number 1 is now the slope, not part of the structural parameter, and only porosity should be treated (powered/multiplied) by the b parameter. Some relationships in the literature are similar to Equation (5) and could also record the utilization of complementary structural parameters n_n, $1-v_m$, and v_f but only in the case of number 1 being outside the powered member and the porosity is powered and also multiplied by another parameter or critical porosity. They include Equation (14) from different sources [34, 40–43] and Equation (15) [12].

$$E_{mn} = E_m \cdot (1 - a \cdot n)^p \tag{14}$$

where the a and p parameters meaning can vary according to chosen source [34, 40–43].

$$E_{mn} = E_m \cdot \left(1 - \frac{n}{n_c}\right)^{\frac{1}{J}} \tag{15}$$

where n_c is critical porosity, while the n_c and J are parameters ensuring the data fitting.

3 | Results and Discussion

3.1 | Observation of Used Materials

The compositions and porosity of matrices are in Table 1. Measured values of mechanical properties of prepared matrices are in tables including Tables 3–6. These tables enable the comparison of the values for real porous matrices and hypothetical nonporous matrices obtained by fitting. The observed values from Tables 3–6 are elastic modulus, ultimate strength, ultimate strain, and energy need for ultimate strength achievement. Particle size distributions (obtained by laser analysis) are

TABLE 2 | Suitability of all possible 10 pairs of structural parameters for research.

Parameter	Suitability or reason for exclusion
$n+n_n$	Nonporous composite: $n+n_n=0$
$n_{fp}+v_f$	Porous matrix: $n_{fp}+v_f=0$
$n_{fp}+n$; $n_{fp}+(1-v_m)$	First fitting: low R^2
$(1-v_m)+n_n$; n_n+v_f; $n_{fp}+n_n$	Slopes values differing according to the used pair of structural parameters
$(1-v_m)+n$; $n+v_f$; $n+(1-v_m)$	Repetition of slope values

Note: Unsuitable pairs were excluded immediately after finding some insufficiency without the whole search for their complex behavior.

in Figure S1, except for the R_2 rubber particle size distribution obtained by sieve analysis due to large particles. 50 wt% of R_2 particles exceeded the size of 2.5 mm. The randomness of the shapes of particles is in Figure S2. The following random microstructure of composites is in Figure S3.

Composites include 10 matrices and six fillers. The calculations are focused only on different matrices. The reason is that three fillers (all inorganic) are included in matrices. The fractions of rubber filler (R_0, R_1, and R_2) embody only low differences in particle sizes—about one mathematical order. This difference seems insufficient for study on their influence on proposed relationships. Moreover, the weak differences enabled including all rubber fractions into one filler in calculations (in each prepared sample was only one from the mentioned fractions).

3.2 | Data Fitting and Numerical Relationships Between Obtained Parameters

Complementary structural parameters can be derived easily from the basic structural parameters. A suitable example is Equation (9), showing the relationship ($n_n=1-n_p$) between the interspace filling (n_p) and the interspace porosity (n_n) as its opposite. The same equation shape serves for the replacement of the basic parameters to complementary parameters in the direction shown by arrows: $1-v_f \rightarrow v_f$, $1-v_m \rightarrow v_m$, $n_{pf} \rightarrow n_{fp}$, and $1-n \rightarrow n$.

Like basic structural parameters, the complementary structural parameters are in the fitting equations used in pairs. There are similarly able to describe the composition of material from two chosen parameters [32, 33].

Each complementary parameter (n_n, $1-v_m$, v_f, n, and n_{pf}) is equal to zero for nonporous matrix, and its value is between 0 and 1 for more complex materials. The exceptions are the zero value for v_f and n_{fp} in the case of porous matrix and n_n and n for nonporous composite. The mentioned zero values lead to different equation types using complementary structural parameters in the fitting. The spatial exponential function [32, 33], represented by Equation (16), is inappropriate because the complementary parameters p_1 or p_2 cannot be zero in it. The whole right side of the equation is then equal to zero in the case of nonporous matrix (always) and in the case of nonporous composite or porous matrix too (according to the choice of pair of complementary parameters as is described at the beginning of this paragraph). The whole equation then has no meaning because $z_c \neq 0$. The right side of Equation (16) should embody non-zero values in the case of porous composite. Despite this, the equation loses its universality in the possibility of its progressive assembly while the material is becoming more complex. The suitable shape for the fitting based on complementary structural parameters is the spatial linear function described by Equation (17).

$$z_c = z_m \cdot p_1^b \cdot p_2^c \tag{16}$$

$$z_c = z_m + z_m \cdot \left(b \cdot p_1 + c \cdot p_2\right) \tag{17}$$

where the meaning of z_c, z_m, b, and c corresponds to members in the Equations (1–3) respectively, Equation (16), and the remaining members are complementary structural parameters. Parameters p_1 and p_2 are signs in their general form. The mathematical relationships among equation members vary from those in Equations (1–3). Fitting members (b, c) are multipliers (instead of exponents), and between structural parameters is plus instead of multiplication. The value of the nonporous matrix property is not only the slope but moreover a displacement from the diagram beginning on the positive part of y-axis. The nonporous matrix property (elastic modulus, etc.) retains the slope meaning because of the necessity to join the matrix mechanical behavior directly with the composition of more complex materials.

There is no problem with zero values of complementary parameters p_1 and p_2 for nonporous matrix—Equation (17) changes its shape to $z_c=z_m+0$, which is existing equality (value for nonporous matrix in both sides of the equation). Moreover, there is no problem with zero values of parameters p_1 and p_2 for nonporous composite and porous matrix—one of the parameters can be zero, and the right side is still not equal to zero or only z_m. There are exceptions shown in Table 2, but Equation (17) combined with suitable pairs of complementary parameters has universality in progressive assembly while the material is becoming more complex. The overview of the suitability of structural parameter pairs for fitting Equation (17) is in Table 2. The studied types of Equation (17) include Equations (18–23) and come from the suitability of complementary parameters shown in this table.

$$z_c = z_m + z_m \cdot \left(b \cdot n_{fp} + c \cdot n_n\right) \tag{18}$$

$$z_c = z_m + z_m \cdot \left(b \cdot \left(1 - v_m\right) + c \cdot n_n\right) \tag{19}$$

$$z_c = z_m + z_m \cdot \left(b \cdot n_n + c \cdot v_f\right) \tag{20}$$

$$z_c = z_m + z_m \cdot \left(b \cdot \left(1 - v_m\right) + c \cdot v_f\right) \tag{21}$$

$$z_c = z_m + z_m \cdot \left(b \cdot n + c \cdot \left(1 - v_m\right)\right) \quad (22)$$

$$z_c = z_m + z_m \cdot \left(b \cdot n + c \cdot v_f\right) \quad (23)$$

There was found no exact mathematical reason why b and c have the form of multipliers of the structural parameters and not as their exponents. The equation form choice was according to the ability to fit the measured data. The general shape of the function is in Equations (24 and 25). These equations depict the possible mathematical treatment of Equation (17):

$$z_c = z_m + z_m \cdot \left(b \cdot p_1 + c \cdot p_2\right) = z_m - z_m \cdot \left(-b \cdot p_1 - c \cdot p_2\right) \quad (24)$$

$$z_c = z_m \cdot \left(1 + \left(b \cdot p_1 + c \cdot p_2\right)\right) = z_m \cdot \left(1 - \left(-b \cdot p_1 + \left(-c \cdot p_2\right)\right)\right) \quad (25)$$

It is necessary to add that the b and c parameters can acquire positive or negative values in both cases of slope sign. It means that, for example, a combination of a negative slope with two positive parameter values, two negative parameter values, or one positive and one negative parameter value according to the chosen fitting example (property and matrix, explained below). When the slope changes its sign, the signs of parameter values also change. It is only a mathematical treatment shown by Equation (24).

The left-placed version of Equation (24) corresponds to Equation (17) which represents the only equation shape in this work. Equation (25) corresponds to Equation (24) after mathematical deriving by pointing the z_m value out.

The data fitting used the form of an adjustment of the b and c values. It was provided separately for each chosen property, and a set of composites based on one from the used matrices. The filler was the same in all cases. Fitting was used for one property and one matrix in the composite as shown in Figure 2. The fitting was concerned with reaching the highest coefficient of determination (R^2) value. All combinations of b and c values embodying the highest R^2 value for separate fitting created a trend with a linear dependence of c on b. On that line, there were two combinations of b and c parameter values differing only by the b and c mathematical sign ensuring the same absolute value of slope and displacement. The resulting slope value then varies only in the mathematical positivity/negativity of its value and the result dependence, as depicted in Figure 2 and Equations (17–23) for the case of the positive slope. The results giving the positive slope were the only ones included in the following work. Figure 2 shows the typical difference between slope and displacement caused by the method used (usually the third valid numeral). The fitting results (for chosen structural pairs) in the form of displacements values are in Table 3 for E, Table 4 for $\sigma_{m,Fmax}$, Table 5 for $\varepsilon_{m,Fmax}$, and Table 6 for $A_{m,Fmax}$. There are also the property values for real porous matrices and porosity to estimate obtained results (the accurate comparison is unsuitable due to the absence of real nonporous matrices).

Ten potentially suitable pairs of structure parameters are already mentioned in Table 2. Only six pairs corresponding to Equations (18–23) were used for fitting ($n_{fp}+n_n$, n_n+1-v_m, n_n+v_f, $1-v_m+v_f$, $n+1-v_m$, and $n+v_f$). The process leads to interesting relationships among the b and c parameters. There were found dependencies in each equation in the form of linear dependence:

$$c = x + y \cdot b \rightarrow z_c = z_m + z_m\left(b \cdot p_1 + (x + y \cdot b) \cdot p_2\right) \quad (26)$$

where x is displacement and y is the slope of c dependence on b. This dependence is then installed instead of the c multiplier to Equation (17), as shown in the following part of Equation (26). The obtained dependencies for each proven combination of structural parameters and observed properties are in Table 7.

Moreover, there are linear dependencies of b and c multipliers across different Equations (18–23) when all relationships belong to one observed property. The equation can acquire more forms:

$$b; c = f(b; c; b + c; b - c) \quad (27)$$

where b or c on the left side belongs to one equation from Equations (18–23), and the random multiplier or sum of multipliers on the right side belongs to another random equation from Equations (18–23). Both multipliers come from one equation from (Equations 18–23) if the sum is on the ride side of Equation (27). Very high values of coefficient of determination R^2 were observed in dependencies of b/c on b/c created from b and c coming from E fitting (nearly 1). The variously worse results occur after the fitting in the cases of the other properties. If there is dependence generally of one multiplier on the sum of multipliers, any dependencies are very rare, but some examples exist. The result is plenty of more or less good linear dependencies. However, some cases are even without any found relationship. There is no reason to show them instead of the dependencies of b on c closed in certain equations depicted in Table 7. However, there is a reason to show some exceptional equations from the plenty of relationships. The chosen relationships have the simple shape $y=x$ or $y=-x$, and their R^2 equals 1 or it is only a little lower. The very significant thing is that the chosen relationships connect all of the b and c members of only three equations including Equations (21–23) mathematically together, and there it is no other exact relationships coming from Equations (18–20). The linear dependencies of b and c across Equations (21–23) work after fitting in cases of all properties by the same mean. The better way to express most of these relationships is by simplifying the material to a nonporous composite (n; $n_n=0$, remaining parameters reduced to v_f) or porous matrix (n_{fp}; $v_f=0$, remaining parameters reduced to n). These expressions (and the addition of relationships without the ability to be shown by material with reduced composition) of b and c connections are in Table 8. This table shows the close connection among the Equations (21–23). Their close relationship can be seen even in Tables 3–6, with very similar values of displacements coming from fitting (nearly equal).

3.3 | Interpolation of b and c Parameters Obtained by Fitting

The b and c parameters in each equation or across different equations have mathematical connections, but this is not important without further interpolations giving them clear meaning. The work led to the finding of dependencies of b and c on matrix

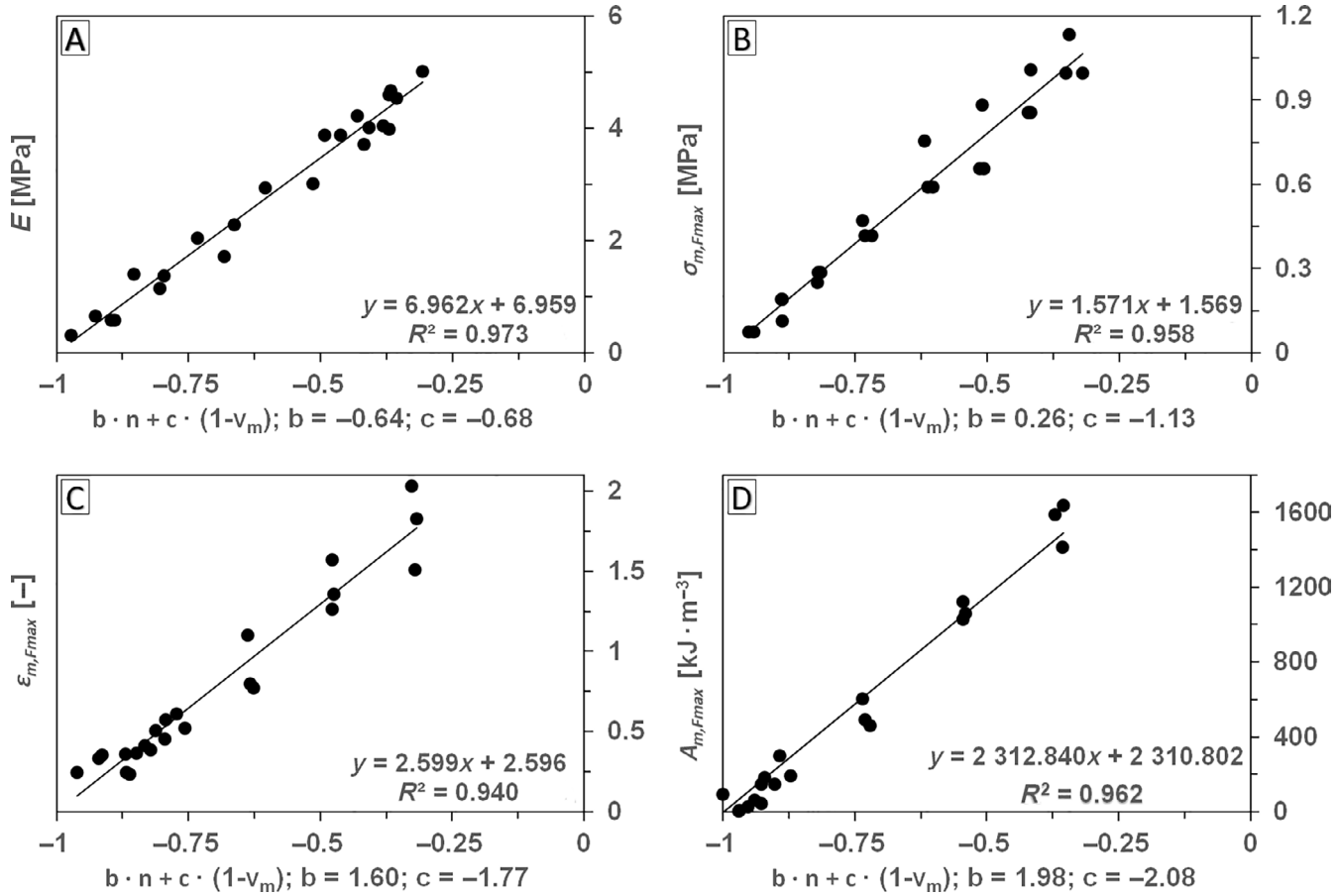

FIGURE 2 | A linear fitting example of observed mechanical properties including E (A), σ_{Fmax} (B), ε_{Fmax} (C), and A_{Fmax} (D) of porous composites based on P_{72}-G_{18}-Ca_{10} matrix and different fractions of rubber fitted according to expression $b \cdot n + c \cdot (1 - v_m)$ leading to Equation (22). The other linear fittings leading to Equations (18–21) and (23) are in the same way.

TABLE 3 | Comparison of elastic modulus values of individual matrices between measured values of real porous matrices with mentioned porosities [32, 33] and values obtained by Equations (18–23) represented by given pairs of structural parameters.

	Measured values (porous matrices)		E (MPa): fitted values of (nonporous matrices), if the structural parameters p_1 and p_2 are					
Matrix designation	n (%)	E (MPa)	$n_{fp}; n_n$	$1-v_m; n_n$	$n_n; v_f$	$1-v_m; v_f$	$n; v_f$	$n; 1-v_m$
P_{99}-W_1	57 ± 7	1.4 ± 0.3	6.65	4.69	5.98	8.85	8.78	8.80
P_{99}-W_1	16 ± 2	4.1 ± 0.1						
P_{95}-G_5	9.5 ± 0.7	13 ± 2	11.38	16.10	12.52	14.94	15.13	14.99
P_{80}-G_{20}	10 ± 1	4.8 ± 0.3	4.65	5.31	4.87	5.54	5.54	5.54
P_{85}-G_5-CO_{10}	2 ± 2	2.3 ± 0.3	2.15	1.69	1.97	2.49	2.50	2.49
P_{65}-CO_{35}	4 ± 1	1.6 ± 0.4	2.22	1.63	2.00	2.58	2.60	2.61
P_{49}-CO_{26}-LO_{25}	1 ± 2	1.1 ± 0.03	1.07	0.81	0.96	1.22	1.25	1.24
P_{33}-CO_{17}-Si_{50}	16 ± 1	9 ± 1	12.39	13.12	12.47	15.15	15.14	15.17
P_{33}-CO_{17}-Ca_{50}	32 ± 2	4.9 ± 0.5	10.20	11.72	10.55	12.90	12.90	12.90
P_{33}-CO_{17}-Fe_{50}	22.6 ± 0.5	9.1 ± 0.6	14.96	16.66	15.46	18.41	18.41	18.44
P_{72}-G_{18}-Ca_{10}	16.3 ± 0.6	7.4 ± 0.8	5.83	6.51	6.03	6.96	6.94	6.96[a]

[a]Depicted in Figure 2.

TABLE 4 | Comparison of ultimate strength values of individual matrices between measured values of real porous matrices with mentioned porosities [32, 33] and values obtained by Equations (18–23) represented by given pairs of structural parameters.

Matrix designation	Measured values (porous matrices)		σ_{Fmax} (MPa): fitted values of (nonporous matrices), if the structural parameters p_1 and p_2 are					
	n (%)	σ_{Fmax} (MPa)	$n_{fp}; n_n$	$1-\nu_m; n_n$	$n_n; \nu_f$	$1-\nu_m; \nu_f$	$n; \nu_f$	$n; 1-\nu_m$
P_{99}-W_1	57 ± 7	0.56 ± 0.05	2.03	2.23	2.06	2.90	2.87	2.89
P_{99}-W_1	16 ± 2	2.7 ± 0.3						
P_{95}-G_5	9.5 ± 0.7	4.7 ± 0.1	2.76	4.33	3.26	3.71	3.74	3.68
P_{80}-G_{20}	10 ± 1	1.75 ± 0.08	1.25	1.46	1.32	1.45	1.45	1.45
P_{85}-G_5-CO_{10}	2 ± 2	1.24 ± 0.04	1.01	1.02	1.02	1.15	1.14	1.14
P_{65}-CO_{35}	4 ± 1	0.42 ± 0.03	0.47	0.37	0.43	0.54	0.54	0.54
P_{49}-CO_{26}-LO_{25}	1 ± 2	0.4 ± 0.03	0.30	0.25	0.27	0.32	0.32	0.32
P_{33}-CO_{17}-Si_{50}	16 ± 1	2.2 ± 0.3	2.57	3.32	2.81	3.22	3.22	3.22
P_{33}-CO_{17}-Ca_{50}	32 ± 2	0.7 ± 0.04	1.14	1.21	1.16	1.41	1.41	1.41
P_{33}-CO_{17}-Fe_{50}	22.6 ± 0.5	1.09 ± 0.09	1.37	1.55	1.44	1.68	1.68	1.68[a]
P_{72}-G_{18}-Ca_{10}	16.3 ± 0.6	1.93 ± 0.06	1.33	1.61	1.43	1.57	1.57	1.57[a]

[a]Depicted in Figure 2.

TABLE 5 | Comparison of ultimate strain values of individual matrices between measured values of real porous matrices with mentioned porosities [32, 33] and values obtained by Equations (18–23) represented by given pairs of structural parameters.

Matrix designation	Measured values (porous matrices)		ε_{Fmax} (%): fitted values of (nonporous matrices), if the structural parameters p_1 and p_2 are					
	n (%)	ε_{Fmax} (%)	$n_{fp}; n_n$	$1-\nu_m; n_n$	$n_n; \nu_f$	$1-\nu_m; \nu_f$	$n; \nu_f$	$n; 1-\nu_m$
P_{99}-W_1	57 ± 7	94 ± 9	114	167	130	153	151	153
P_{99}-W_1	16 ± 2	82 ± 12						
P_{95}-G_5	9.5 ± 0.7	140 ± 40	99	130	111	124	125	124
P_{80}-G_{20}	10 ± 1	340 ± 20	328	462	374	367	367	367
P_{85}-G_5-CO_{10}	2 ± 2	100 ± 4	141	165	149	154	154	154
P_{65}-CO_{35}	4 ± 1	39 ± 4	40	36	39	41	41	41
P_{49}-CO_{26}-LO_{25}	1 ± 2	68 ± 8	52	50	51	53	53	52
P_{33}-CO_{17}-Si_{50}	16 ± 1	22 ± 1	22	23	22	23	23	23
P_{33}-CO_{17}-Ca_{50}	32 ± 2	20 ± 1	19	18	18	19	19	19
P_{33}-CO_{17}-Fe_{50}	22.6 ± 0.5	13 ± 1	14	15	15	14	14	14
P_{72}-G_{18}-Ca_{10}	16.3 ± 0.6	260 ± 30	224	315	255	260	260	260[a]

[a]Depicted in Figure 2.

properties only because only one type of filler was used (instead of 10 various matrices). The interpolation possibilities differ according to the observed property. This result should depend on the relationships between b and c coming from fitting. The graphical examples of interpolation are in figures including Figures 3–8. All interpolation results are in tables including Tables 9–12 that serve as interpolation overviews for separated observed properties. Two interpolation possibilities are for the b and c parameters if the observed property is elastic modulus. The interpolation by expression $E_m \cdot \delta$ gives the generally higher R^2 than only the E_m (elastic modulus value of matrix) independently of the choice of structural parameters pair. The resulting interpolation is shown by Equation (28) if the structural parameters are written generally as p_1 and p_2, and the choice is according to the value of R^2.

$$E_c = E_m + E_m \cdot \left(\left(d + e \cdot \ln\left(E_m \cdot \delta\right)\right) \cdot p_1 + \left(f + g \cdot \ln\left(E_m \cdot \delta\right)\right) \cdot p_2\right) \quad (28)$$

TABLE 6 | Comparison of energy need for ultimate strength achievement values of individual matrices between measured values of real porous matrices with mentioned porosities [32, 33] and values obtained by Equations (18–23) represented by given pairs of structural parameters.

Matrix designation	Measured values (porous matrices)		A_{Fmax} (kJ m^{-3}): fitted values of (nonporous matrices), if the structural parameters p_1 and p_2 are					
	n (%)	A_{Fmax} (kJ m^{-3})	$n_{fp}; n_n$	$1-v_m; n_n$	$n_n; v_f$	$1-v_m; v_f$	$n; v_f$	$n; 1-v_m$
P_{99}-W_1	57 ± 7	321 ± 14	881	1243	974	1315	1309	1318
P_{99}-W_1	16 ± 2	1400 ± 400						
P_{95}-G_5	9.5 ± 0.7	4100 ± 700	1423	2478	1757	1965	1986	1946
P_{80}-G_{20}	10 ± 1	3700 ± 300	2450	3593	2841	2749	2748	2748
P_{85}-G_5-CO_{10}	2 ± 2	700 ± 50	733	895	793	826	825	825
P_{65}-CO_{35}	4 ± 1	69 ± 6	132	92	119	147	149	150
P_{49}-CO_{26}-LO_{25}	1 ± 2	90 ± 8	86	81	84	93	94	93
P_{33}-CO_{17}-Si_{50}	16 ± 1	210 ± 40	258	325	279	325	325	325
P_{33}-CO_{17}-Ca_{50}	32 ± 2	69 ± 9	114	128	116	147	146	147
P_{33}-CO_{17}-Fe_{50}	22.6 ± 0.5	70 ± 10	105	126	112	131	131	131
P_{72}-G_{18}-Ca_{10}	16.3 ± 0.6	3700 ± 300	1958	2942	2299	2311	2311	2311[a]

[a]Depicted in Figure 2.

All interpolation possibilities of b and c parameters in the case of E are in Table 9 for all fitting Equations (18–23). The examples of interpolations coming from Equation (22) are in Figure 3. All interpolations lead to logarithmic functions.

Four interpolation types of the b and c parameters are possible if the observed property is the ultimate strength. Most simple interpolation done only by $\sigma_{m,Fmax}$ gives the lowest R^2 values. The multiplication of $\sigma_{m,Fmax}$ by δ or $S_{m,rel}$, or using both extra variables δ (as a multiplier) or $S_{m,rel}$ (as a divisor) can improve the interpolation. The interpolation by expression $\sigma_{m,Fmax} \cdot \delta / S_{m,rel}$ gives mostly the highest R^2 (with some exceptions of interpolation by $\sigma_{m,Fmax} \cdot \delta$ *and* $\sigma_{m,Fmax} \cdot S_{m,rel}$). $S_{m,rel}$ values were obtained from Equation (8). Values for $S_{m,rel}$ calculation in Equation (8), including $\sigma_{m,Fmax}$, $\varepsilon_{m,Fmax}$, and $A_{m,Fmax}$, were from Tables 4–6. Each b and c parameter interpolation (from any equation) is independent. The resulting interpolation equations then acquire a lot of types due to the many possibilities of their interpolation. Therefore, only the most successful cases of Equations (18–23) are shown. The most common form is (structural parameters are written generally as p_1 and p_2):

$$\sigma_{c,Fmax} = \sigma_{m,Fmax} + \sigma_{m,Fmax} \cdot \left(\left(d + e \cdot \ln \frac{\sigma_{m,Fmax} \cdot \delta}{S_{m,rel}} \right) \cdot p_1 + \left(f + g \cdot \ln \frac{\sigma_{m,Fmax} \cdot \delta}{S_{m,rel}} \right) \cdot p_2 \right) \quad (29)$$

if $p_1 = 1 - v_m$ and $p_2 = v_f$, it is the best some other interpolation:

$$b = d + e \cdot \ln \frac{\sigma_{m,Fmax} \cdot \delta}{S_{m,rel}}; \quad c = f + g \cdot \ln\left(\sigma_{m,Fmax} \cdot \delta\right) \quad (30)$$

if $p_1 = n$ and $p_2 = 1 - v_m$, it is the best some other interpolation:

$$b = d + e \cdot \ln\left(\sigma_{m,Fmax} \cdot \delta\right); \quad c = f + g \cdot \ln\left(\sigma_{m,Fmax} \cdot S_{m,rel}\right) \quad (31)$$

and if $p_1 = n$ and $p_2 = v_f$, it is the best some other interpolation:

$$b = d + e \cdot \ln \frac{\sigma_{m,Fmax} \cdot \delta}{S_{m,rel}}; \quad c = f + g \cdot \ln\left(\sigma_{m,Fmax} \cdot S_{m,rel}\right) \quad (32)$$

Equations (30–32) embody only a weak advantage against the interpolation presented by Equation (29). The interpolation possibilities overview if the observed property is the ultimate strength is in Table 10. The graphical overview for the case if the structural parameters are n and $1 - v_m$ is in Figures 4 and 5.

Three interpolation types of the b and c parameters are possible if the observed property is the ultimate strain. The interpolation by expression $\varepsilon_{m,Fmax} \cdot \delta$ gives mostly the highest R^2 with some exceptions of interpolation by δ. The interpolation only according to simple $\varepsilon_{m,Fmax}$ is possible and is more appropriate than δ in many cases (not all), while it is also worse than $\varepsilon_{m,Fmax} \cdot \delta$. Each b and c parameter interpolation (from any equation) is independent. The resulting interpolation equations then can acquire a lot of types due to many possibilities of how to interpolate them. Therefore, only the most successful cases of Equations (18–23) are shown. The most appropriate forms are (structural parameters are written generally as p_1 and p_2):

$$\varepsilon_{c,Fmax} = \varepsilon_{m,Fmax} + \varepsilon_{m,Fmax} \cdot \left(\left(d + e \cdot \ln\left(\varepsilon_{m,Fmax} \cdot \delta\right) \right) \cdot p_1 + \left(f + g \cdot \ln\left(\varepsilon_{m,Fmax} \cdot \delta\right) \right) \cdot p_2 \right) \quad (33)$$

if the pair of structural parameters $p_1 + p_2$ is $(1 - v_m) + n_n$ or $n + 1 - v_m$.

$$\varepsilon_{c,Fmax} = \varepsilon_{m,Fmax} + \varepsilon_{m,Fmax} \cdot \left(\left(d + e \cdot \ln\left(\varepsilon_{m,Fmax} \cdot \delta\right) \right) \cdot p_1 + \left(f + g \cdot \ln \delta \right) \cdot p_2 \right) \quad (34)$$

if the pair of structural parameters $p_1 + p_2$ is $n_{fp} + n_n$.

$$\varepsilon_{c,Fmax} = \varepsilon_{m,Fmax} + \varepsilon_{m,Fmax} \cdot \left(\left(d + e \cdot \ln \delta \right) \cdot p_1 + \left(f + g \cdot \ln\left(\varepsilon_{m,Fmax} \cdot \delta\right) \right) \cdot p_2 \right) \quad (35)$$

TABLE 7 | Dependencies of structural parameters c and b in the form of $c = f(b)$ in Equations (18–23) in cases of different properties fitting (E, σ_{Fmax}, ε_{Fmax} respectively A_{Fmax}) with the attached coefficient of determination (R^2) values.

Property	$p_1 + p_2$ (in $b \cdot p_1 + c \cdot p_2$)[a]	Eq.	$c = f(b)$	$c = f(b)$; R^2
E	$n_{fp} + n_n$	(18)	$c = -0.864 \cdot b - 1.101$	0.994
	$(1 - v_m) + n_n$	(19)	$c = -0.962 \cdot b - 1.061$	0.998
	$n_n + v_f$	(20)	$c = -2.431 \cdot b - 2.646$	0.980
	$(1 - v_m) + v_f$	(21)	$c = -2.529 \cdot b - 2.323$	0.995
	$n + (1 - v_m)$	(22)	$c = -0.574 \cdot b - 1.097$	0.997
	$n + v_f$	(23)	$c = -1.333 \cdot b - 2.550$	0.983
σ_{Fmax}	$n_{fp} + n_n$	(18)	$c = -0.870 \cdot b - 1.074$	0.978
	$(1 - v_m) + n_n$	(19)	$c = -0.991 \cdot b - 1.047$	0.993
	$n_n + v_f$	(20)	$c = -2.301 \cdot b - 2.483$	0.939
	$(1 - v_m) + v_f$	(21)	$c = -2.295 \cdot b - 2.410$	0.961
	$n + (1 - v_m)$	(22)	$c = -0.580 \cdot b - 1.081$	0.990
	$n + v_f$	(23)	$c = -1.314 \cdot b - 2.483$	0.940
ε_{Fmax}	$n_{fp} + n_n$	(18)	$c = -0.603 \cdot b - 0.282$	0.872
	$(1 - v_m) + n_n$	(19)	$c = -0.611 \cdot b - 0.249$	0.895
	$n_n + v_f$	(20)	—	—
	$(1 - v_m) + v_f$	(21)	—	—
	$n + (1 - v_m)$	(22)	$c = -0.819 \cdot b - 0.414$	0.876
	$n + \mathrm{v_f}$	(23)	—	—
A_{Fmax}	$n_{fp} + n_n$	(18)	$c = -0.960 \cdot b - 1.151$	0.986
	$(1 - v_m) + n_n$	(19)	$c = -1.020 \cdot b - 1.091$	0.995
	$n_n + v_f$	(20)	$c = -1.908 \cdot b - 2.201$	0.946
	$(1 - v_m) + v_f$	(21)	$c = -2.057 \cdot b - 2.223$	0.978
	$n + (1 - v_m)$	(22)	$c = -0.523 \cdot b - 1.065$	0.985
	$n + v_f$	(23)	$c = -1.062 \cdot b - 2.199$	0.936

[a]There are also shown pairs of structural parameters in the Equations (18–23) generally shaped as $z_c = z_m + z_m \cdot (b \cdot p_1 + c \cdot p_2)$.

if the pair of structural parameters $p_1 + p_2$ is $n_n + v_f$, $(1 - v_m) + v_f$ or $n + v_f$. The dependence $c = f(\varepsilon_{m,Fmax})$ is also good in these cases. Functions coming from interpolation are in Table 11, serving as an interpolation overview for interpolation related to ε_{Fmax}. The possibilities of interpolation if the pair of structural parameters is $n + 1 - v_m$ are in Figure 6.

There are six possibilities ($A_{m,Fmax}$, $A_{m,Fmax} \cdot \delta$, δ, $\varepsilon_{m,Fmax}$, $\varepsilon_{m,Fmax} \cdot \delta$ and $\sigma_{m,Fmax} \cdot \delta$), how to interpolate the b and c parameters if the observed property is A_{Fmax}. Usually is better to combine the δ with any property. $\sigma_{m,Fmax}$ seems inappropriate for interpolation without δ against $\varepsilon_{m,Fmax}$, and $A_{m,Fmax}$. The most appropriate cases are (structural parameters are written generally as p_1 and p_2):

$$A_{c,Fmax} = A_{m,Fmax} + A_{m,Fmax} \cdot \left(\left(d + e \cdot \ln\left(A_{m,Fmax} \cdot \delta \right) \right) \cdot p_1 + \left(f + g \cdot \ln\left(A_{m,Fmax} \cdot \delta \right) \right) \cdot p_2 \right) \quad (36)$$

except for the situation if the pair of structural parameters $p_1 + p_2$ is $(1\text{-}v_m) + n_n$.

$$A_{c,Fmax} = A_{m,Fmax} + A_{m,Fmax} \cdot \left(\left(d + e \cdot \ln\left(\sigma_{m,Fmax} \cdot \delta \right) \right) \cdot p_1 + \left(f + g \cdot \ln\left(\sigma_{m,Fmax} \cdot \delta \right) \right) \cdot p_2 \right) \quad (37)$$

Functions coming from interpolation are in Table 12, which serves as an interpolation overview for interpolations related to A_{Fmax}. The possibilities of interpolation if the pair of structural parameters is $n + 1 - v_m$ are in Figures 7 and 8.

There are many d, e, f, and g parameters in the equations shown in Tables 9–12. What is their function or meaning? The assumption is that parameters d, e, f, and g in the equations should vary according to the pair of filler and matrix in composites. These parameters are the last members in equations without proven meaning and description. On the other hand, the properties and behavior of fillers, their influence on material porosity, and other material properties are the undescribed parts of the composite material description in this work. Therefore, there is an assumption to join parameters d,

TABLE 8 | The mathematical behavior of pairs of structural parameters and their multipliers coming from the Equations (21–23) in simplified situations of less complex materials.

Porous composite (the examples of fitting results of Equations (21–23)) from up to down			
$\sigma_{c,Fmax}\,(\mathrm{MPa}) = 3.71\,\mathrm{MPa} + 3.69\,\mathrm{MPa} \cdot (-0.91 \cdot (1-v_m) - 0.42 \cdot v_f)$			
$\sigma_{c,Fmax}\,(\mathrm{MPa}) = 3.68\,\mathrm{MPa} + 3.68\,\mathrm{MPa} \cdot (0.35 \cdot n - 1.29 \cdot (1-v_m))$			
$\sigma_{c,Fmax}\,(\mathrm{MPa}) = 3.74\,\mathrm{MPa} + 3.73\,\mathrm{MPa} \cdot (-0.91 \cdot n - 1.34 \cdot v_f)$			
Multiplied parameters	**Mathem. treatment**	**Multipliers behavior (Eq.)**	**Notice**
Hypothetical nonporous composite			
$-0.91 \cdot (1\text{-}v_m) - 0.42 \cdot v_f$	$-1.33 \cdot v_f$	$b + c\,(21) = c\,(22) = c\,(23)$	$1 - v_m = v_f$
$0.35 \cdot n - 1.29 \cdot (1-v_m)$	$-1.29 \cdot v_f$	$c\,(22) = c\,(23) = b + c\,(21)$	$1 - v_m = v_f$, $n = 0$
$-0.91 \cdot n - 1.34 \cdot v_f$	$-1.34 \cdot v_f$	$c\,(23) = b + c\,(21) = c\,(22)$	$n = 0$
Porous matrix			
$-0.91 \cdot (1-v_m) - 0.42 \cdot v_f$	$-0.91 \cdot n$	$b\,(21) = b + c\,(22) = b\,(23)$	$1 - v_m = n$, $v_f = 0$
$0.35 \cdot n - 1.29 \cdot (1-v_m)$	$-0.94 \cdot n$	$b + c\,(22) = b\,(23) = b\,(21)$	$1 - v_m = n$
$-0.91 \cdot n - 1.34 \cdot v_f$	$-0.91 \cdot n$	$b\,(23) = b\,(21) = b + c\,(22)$	$v_f = 0$
Further relationships found between *b* and *c* multipliers			
$c\,(21) = -b\,(22) = b - c\,(23)$			

Note: The data fittings connecting the composites based on the P_{95}-G_5 matrix and corresponding ultimate strength values serve as an example.

e, *f*, and *g* and fillers properties together, but without accurate description, due to data focusing on different matrices and not focusing on different fillers with their properties and influence on material porosity in this work.

There is a simplification of proposed relationships in case of the material complexity reduction from porous composite to nonporous composite (n; $n_n = 0$, remaining parameters reduced to v_f) or porous matrix (n_{fp}; $v_f = 0$, remaining parameters reduced to n). Equation (17) changes into general Equation (38), and Equations (18–23) changes into Equation (39) for nonporous composite or Equation (40) for porous matrix.

$$z_c = z_m + z_m \cdot b \cdot p \tag{38}$$

$$z_c = z_m + z_m \cdot b \cdot v_f \tag{39}$$

$$z_{mn} = z_m + z_m \cdot b \cdot n \tag{40}$$

where z_{mn} is generally labeled property value valid for porous matrix. Equations (28–37), which contain the results of interpolations, should be simplified too. This approach should be accepted for Equation (39), which is valid (mathematically) for cases of filled composites without porosity. There should also be only two interpolation parameters (labeled *d* and *e* or *f* and *g*) valid for cases of missing porosity in material because of only one fitting parameter—*b*. However, the behavior between matrix and filler can vary seriously because of many kinds of potential matrices and fillers. Equation (39) then assumes generally a lot of different possible relationships between filler and matrix, and two remaining interpolation parameters should vary according to filler and its relation to the matrix.

Therefore, there is also an assumption (or idea) of the extra *d* and *e* parameter values in the case of a porous matrix without filler if there is an assumption of dependence of *d*, *e*, *f*, and *g* on filler properties in composites. The potential interpolation is easy because only the *b* parameter is present in Equation (40), which leads to two interpolation parameters—*d* and *e*. Values of these parameters should exist as interpolation results of *b* parameters of porous matrices if filler absence is as filler type. The reduction of interpolation parameters then should lead to universal interpolation parameters in the case of Equation (40). Parameters *d* and *e* should become numbers in that case. However, there are possible influences of different void shapes on material behavior in the case of filler absence. It is indicated in the literature [40, 42, 43]. On the other hand, there is a question about its relevancy from a macroscopic point of view to the properties of material containing voids negligible in comparison with the dimensions of the material body as is suggested in this work. However, only a limited data set was available, but it was trying to find universal *d* and *e* parameters for Equation (40). The attempt is later. In contrast with Equation (40), the interpolation joined with nonporous composites (Equation 39) was not tried because they were not available.

It is no fitting possibility for porous matrices as in the case of the porous composites because each matrix has only one porosity value (except the P_{99}-W_1 prepared with two porosity values). The process has to be different, and the results should be less accurate. The members of Equation (40) are from various sources. The measured z_{mn} values for porous matrices and fitted z_m values for nonporous matrices from the fitting of data belonging to porous composites are in tables including Tables 3–6 according to chosen property. The porosity value has the origin in Equation (6). The member *b* is the only remaining unknown calculated by known

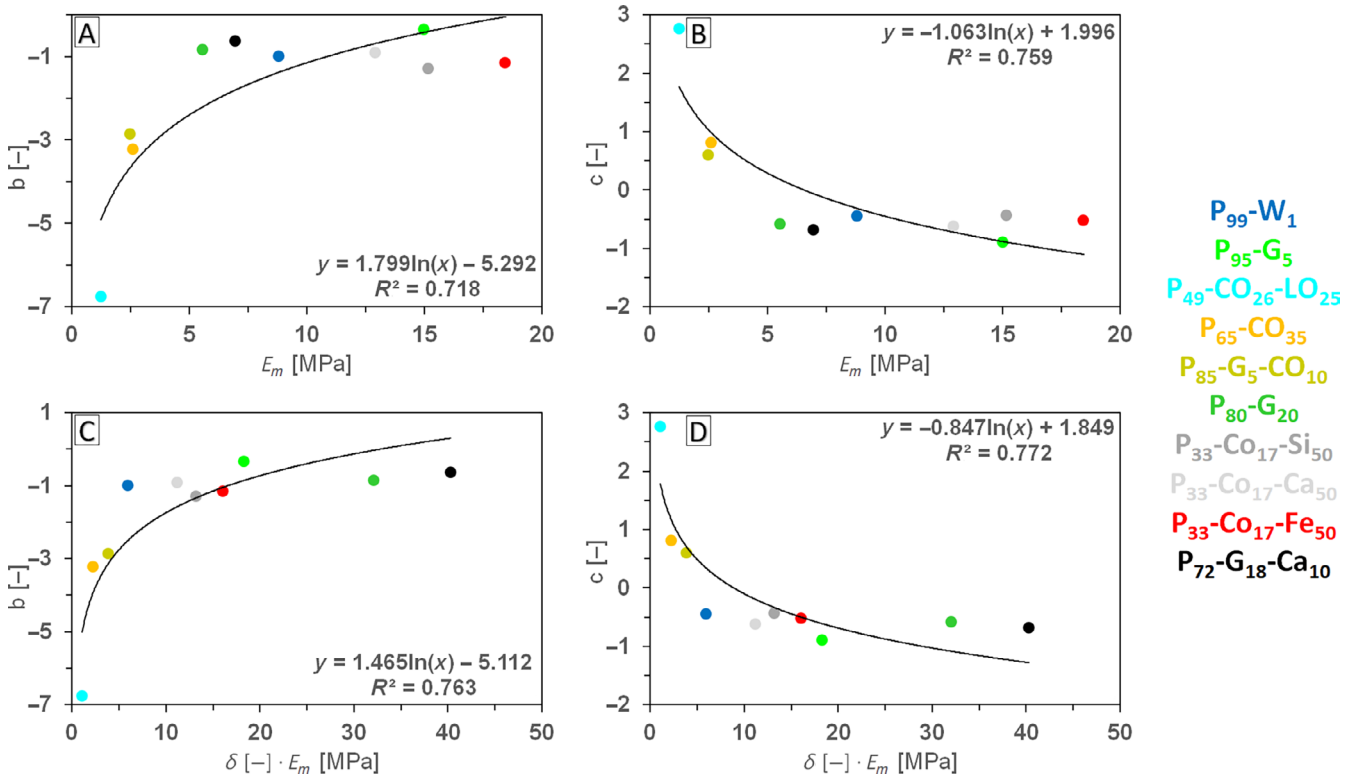

FIGURE 3 | Example of b (A, C) and c (B, D) parameters interpolations coming from fitting Equation (22) $z_c = z_m + z_m \cdot (b \cdot n + c \cdot (1 - v_m))$ derived for elastic modulus according to E_m (A, B) and $E_m \cdot \delta$ (C, D), where E_m values are from Table 3 and δ values are from Table 1. [Color figure can be viewed at wileyonlinelibrary.com]

TABLE 9 | Interpolation possibilities of b and c parameters from Equations (18–23) with general shape $z_c = z_m + z_m \cdot (b \cdot p_1 + c \cdot p_2)$ for elastic modulus according to E_m and $E_m \cdot \delta$, where E_m [MPa] values are from Table 3 and δ values from Table 1.

Eq.	$p_1 + p_2$	$b = f(x); x = E_m \cdot \delta$	R^2	$c = f(x); x = E_m \cdot \delta$	R^2
(18)	$n_{fp} + n_n$	$b = -1.130 \cdot \ln x + 2.284$	0.795	$c = 0.983 \cdot \ln x - 3.535$	0.786
(19)	$(1 - v_m) + n_n$	$b = -1.359 \cdot \ln x + 3.346$	0.879	$c = 1.311 \cdot \ln x - 4.287$	0.881
(20)	$n_n + v_f$	$b = 0.451 \cdot \ln x - 2.203$	0.822	$c = -1.112 \cdot \ln x + 2.742$	0.829
(21)	$(1 - v_m) + v_f$	$b = 0.638 \cdot \ln x - 3.315$	0.741	$c = -1.505 \cdot \ln x + 5.224$	0.760
(22)	$n + (1 - v_m)$	$b = 1.465 \cdot \ln x - 5.112$[a]	0.763	$c = -0.847 \cdot \ln x + 1.849$[a]	0.772
(23)	$n + v_f$	$b = 0.611 \cdot \ln x - 3.244$	0.741	$c = -0.839 \cdot \ln x + 1.827$	0.772
Eq.	$p_1 + p_2$	$b = f(x); x = E_m$	R^2	$c = f(x); x = E_m$	R^2
(18)	$n_{fp} + n_n$	$b = -1.388 \cdot \ln x + 2.912$	0.711	$c = 1.144 \cdot \ln x - 3.523$	0.642
(19)	$(1 - v_m) + n_n$	$b = -1.679 \cdot \ln x + 3.457$	0.840	$c = 1.588 \cdot \ln x - 4.342$	0.810
(20)	$n_n + v_f$	$b = -0.516 \cdot \ln x - 2.173$	0.647	$c = -1.378 \cdot \ln x + 2.845$	0.767
(21)	$(1 - v_m) + v_f$	$b = 0.761 \cdot \ln x - 3.350$	0.658	$c = -1.847 \cdot \ln x + 5.404$	0.715
(22)	$n + (1 - v_m)$	$b = 1.799 \cdot \ln x - 5.292$[a]	0.718	$c = -1.063 \cdot \ln x + 1.996$[a]	0.759
(23)	$n + v_f$	$b = -0.727 \cdot \ln x - 3.274$	0.653	$c = -1.053 \cdot \ln x + 1.972$	0.757

[a]Dependencies depicted in Figure 3.

members. Equation (40) can have more versions because this equation can have the source of z_m in different Equations (18–23) adapted to the chosen property, so the z_m values are various due to the origin of the equation. It leads to several similar variants of Equation (40) b parameters presented for E and σ_{Fmax}. The b interpolations possibilities are in Table 13. The example based on the $1 - v_m$ and n parameters (also Equation (22)) is in Figure 9. The interpolations of ε_{Fmax} and A_{Fmax} were not successful. There

TABLE 10 | Interpolation possibilities of b and c parameters from Equations (18–23) with general shape $z_c = z_m + z_m \cdot (b \cdot p_1 + c \cdot p_2)$ for ultimate strength according to $\sigma_{m,Fmax}$, $\sigma_{m,Fmax} \cdot S_{m,rel}$, $\sigma_{m,Fmax} \cdot \delta$ and $\sigma_{m,Fmax} \cdot \delta / S_{m,rel}$, where $\sigma_{m,Fmax}$ [MPa] values are from Table 4, δ values from Table 1 and $S_{m,rel}$ from Equation (8).

Eq.	$p_1 + p_2$	$b = f(x); x = \sigma_{m,Fmax}$	R^2	$c = f(x); x = \sigma_{m,Fmax}$	R^2
(18)	$n_{fp} + n_n$	$b = -0.949 \cdot \ln x - 0.225$	0.668	$c = 0.763 \cdot \ln x - 0.868$	0.559
(19)	$(1 - v_m) + n_n$	$b = -1.088 \cdot \ln x - 0.026$	0.817	$c = 1.080 \cdot \ln x - 1.022$	0.816
(20)	$n_n + v_f$	$b = -0.361 \cdot \ln x - 1.004$	0.603	$c = -0.976 \cdot \ln x + 0.145$	0.781
(21)	$(1 - v_m) + v_f$	$b = 0.526 \cdot \ln x - 1.592$	0.673	$c = -1.246 \cdot \ln x + 1.258$	0.689
(22)	$n + (1 - v_m)$	$b = 1.206 \cdot \ln x - 1.237$[a]	0.687	$c = -0.721 \cdot \ln x - 0.355$[a]	0.721
(23)	$n + v_f$	$b = 0.514 \cdot \ln x - 1.579$	0.664	$c = -0.774 \cdot \ln x - 0.372$	0.820
Eq.	$p_1 + p_2$	$b = f(x); x = \sigma_{m,Fmax} \cdot S_{m,rel}$	R^2	$c = f(x); x = \sigma_{m,Fmax} \cdot S_{m,rel}$	R^2
(18)	$n_{fp} + n_n$	$b = -1.145 \cdot \ln x - 0.902$	0.778	$c = 0.938 \cdot \ln x - 0.316$	0.675
(19)	$(1 - v_m) + n_n$	$b = -1.350 \cdot \ln x - 0.840$	0.860	$c = 1.344 \cdot \ln x - 0.213$	0.863
(20)	$n_n + v_f$	$b = 0.457 \cdot \ln x - 0.736$	0.698	$c = -1.207 \cdot \ln x - 0.858$	0.864
(21)	$(1 - v_m) + v_f$	$b = 0.635 \cdot \ln x - 1.182$	0.694	$c = -1.571 \cdot \ln x + 0.264$	0.775
(22)	$n + (1 - v_m)$	$b = 1.536 \cdot \ln x - 0.276$[a]	0.772	$c = -0.926 \cdot \ln x - 0.932$[a]	0.825
(23)	$n + v_f$	$b = 0.620 \cdot \ln x - 1.181$	0.681	$c = -0.946 \cdot \ln x - 0.976$	0.862
Eq.	$p_1 + p_2$	$b = f(x); x = \sigma_{m,Fmax} \cdot \delta$	R^2	$c = f(x); x = \sigma_{m,Fmax} \cdot \delta$	R^2
(18)	$n_{fp} + n_n$	$b = -0.680 \cdot \ln x - 0.062$	0.848	$c = 0.607 \cdot \ln x - 1.027$	0.872
(19)	$(1 - v_m) + n_n$	$b = -0.772 \cdot \ln x + 0.129$	0.834	$c = 0.784 \cdot \ln x - 1.185$	0.870
(20)	$n_n + v_f$	$b = 0.296 \cdot \ln x - 1.081$	0.915	$c = -0.676 \cdot \ln x + 0.003$	0.848
(21)	$(1 - v_m) + v_f$	$b = 0.411 \cdot \ln x - 1.677$	0.885	$c = -0.951 \cdot \ln x + 1.433$	0.862
(22)	$n + (1 - v_m)$	$b = 0.922 \cdot \ln x - 1.418$[b]	0.864	$c = -0.523 \cdot \ln x - 0.265$[b]	0.819
(23)	$n + v_f$	$b = 0.406 \cdot \ln x - 1.655$	0.892	$c = -0.529 \cdot \ln x - 0.298$	0.824
Eq.	$p_1 + p_2$	$b = f(x); x = \sigma_{m,Fmax} \cdot \delta / S_{m,rel}$	R^2	$c = f(x); x = \sigma_{m,Fmax} \cdot \delta / S_{m,rel}$	R^2
(18)	$n_{fp} + n_n$	$b = -0.682 \cdot \ln x + 0.362$	0.867	$c = 0.602 \cdot \ln x - 1.399$	0.873
(19)	$(1 - v_m) + n_n$	$b = -0.729 \cdot \ln x + 0.580$	0.870	$c = 0.737 \cdot \ln x + 1.640$	0.901
(20)	$n_n + v_f$	$b = 0.283 \cdot \ln x - 1.253$	0.917	$c = -0.660 \cdot \ln x + 0.410$	0.884
(21)	$(1 - v_m) + v_f$	$b = 0.391 \cdot \ln x - 1.940$	0.914	$c = -0.885 \cdot \ln x + 2.026$	0.856
(22)	$n + (1 - v_m)$	$b = 0.855 \cdot \ln x - 1.974$[b]	0.858	$c = -0.485 \cdot \ln x + 0.050$[b]	0.813
(23)	$n + v_f$	$b = 0.385 \cdot \ln x - 1.922$	0.922	$c = -0.505 \cdot \ln x + 0.041$	0.861

[a]Dependencies depicted in Figure 4.
[b]Dependencies depicted in Figure 5.

are only hints of dependencies. The possible explanation is the absence of fitting and its replacement by calculations. It is necessary to perceive, that each b parameter arose from the fitted z_m value of composites and measured values of n and z_{mn} representing the low amount of samples (1 set = 5 identical samples). The assumption is its relevancy is lower when compared with the parameter b obtained by fitting several sets of identical samples (different sets = different porosity and sample properties). Therefore, inaccurate results are in Table 13.

Nevertheless, despite this, the obtained results are supposed to be evaluated. The data in Table 13 show different results in the case of E according to the origin of z_m. When the z_m comes from Equations (18–20), Equation (41) is better for an interpolation of the b parameter from Equation (40). Against this, the z_m values from Equations (21–23) lead to Equation (42). The combinations of Equation (42) with Equations (21–23) lead to relatively high R^2 (nearly 0.8) and numerically closed values of d and e parameters (see Table 13). The high R^2 value is important. It would be suitable to increase it. A possible way of getting b parameter values is by fitting several matrices with different (controlled) porosity values (not possible in the case of our matrices)—the same mean as used for composites.

$$b = d + e \cdot \ln E \tag{41}$$

$$b = d + e \cdot \ln(E \cdot \delta) \tag{42}$$

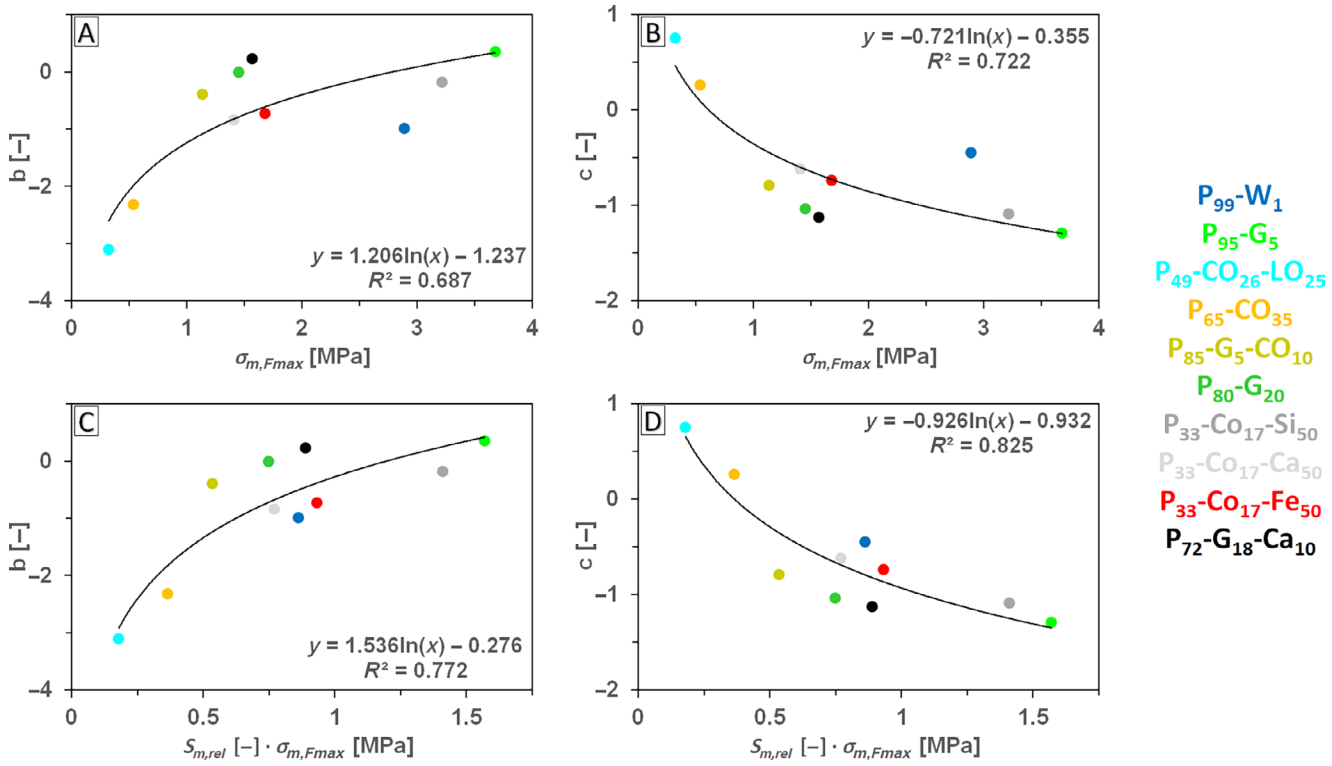

FIGURE 4 | Example of b (A, C) and c (B, D) parameters interpolations coming from fitting Equation (22) $z_c = z_m + z_m \cdot (b \cdot n + c \cdot (1 - v_m))$ derived for ultimate strength according to $\sigma_{m,Fmax}$ (A, B) and $\sigma_{m,Fmax} \cdot S_{m,rel}$ (C, D), where $\sigma_{m,Fmax}$ values are from Table 4 and $S_{m,rel}$ values from Equation (8). [Color figure can be viewed at wileyonlinelibrary.com]

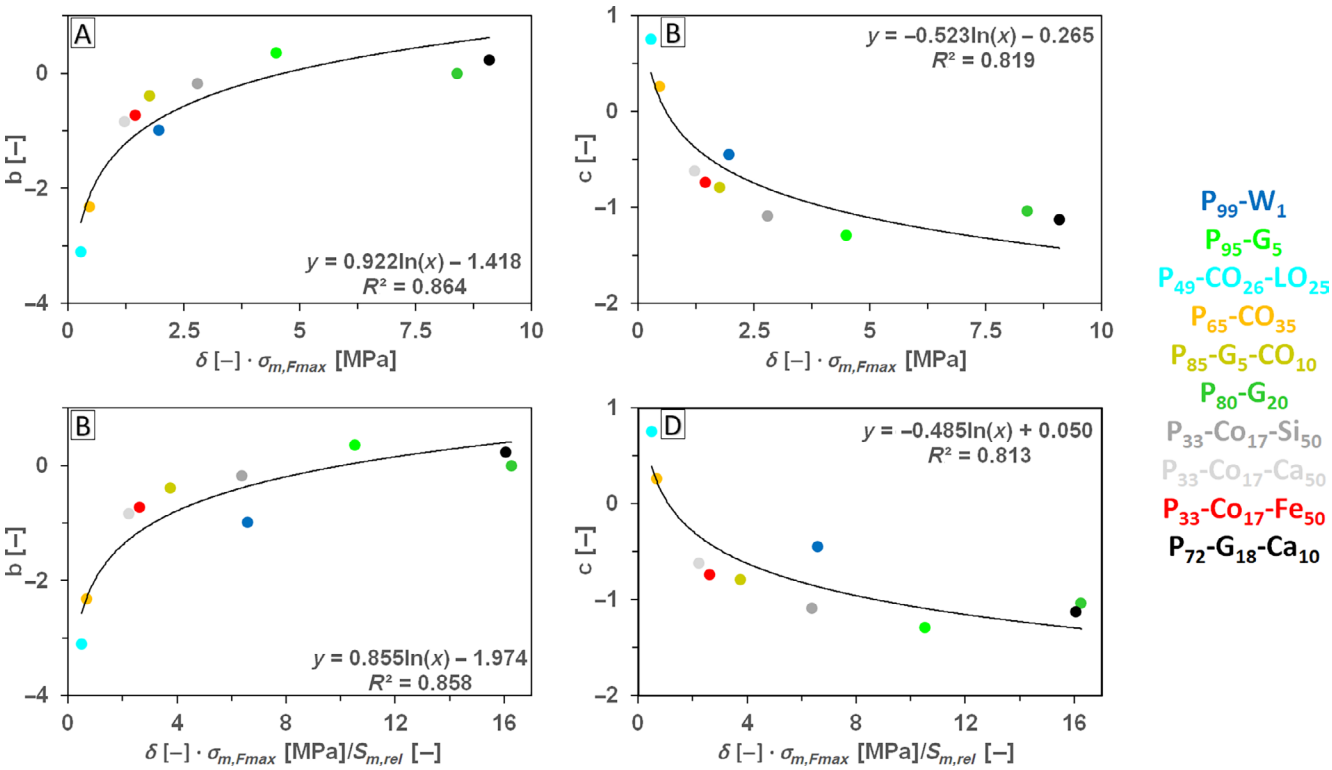

FIGURE 5 | Example of b (A, C) and c (B, D) parameters interpolations coming from fitting Equation (22) $z_c = z_m + z_m \cdot (b \cdot n + c \cdot (1 - v_m))$ derived for ultimate strength according to $\sigma_{m,Fmax} \cdot \delta$ (A, B) and $\sigma_{m,Fmax} \cdot \delta / S_{m,rel}$ (C, D), where $\sigma_{m,Fmax}$ values are from Table 4, δ values are from Table 1 and $S_{m,rel}$ values from Equation (8). [Color figure can be viewed at wileyonlinelibrary.com]

TABLE 11 | Interpolation possibilities of b and c parameters from Equations (18–23) with general shape $z_c = z_m + z_m \cdot (b \cdot p_1 + c \cdot p_2)$ for ultimate strain according to $\varepsilon_{m,Fmax}$, $\varepsilon_{m,Fmax} \cdot \delta$ and δ, where $\sigma_{m,Fmax}$ [MPa] values are from Table 5 and δ values from Table 1.

Eq.	$p_1 + p_2$	$b = f(x); x = \varepsilon_{m,Fmax}$	R^2	$c = f(x); x = \varepsilon_{m,Fmax}$	R^2
(18)	$n_{fp} + n_n$	$b = -0.822 \cdot \ln x - 1.102$	0.860	$c = 0.424 \cdot \ln x + 0.353$	0.550
(19)	$(1 - v_m) + n_n$	$b = -0.676 \cdot \ln x + 0.908$	0.889	$c = 0.372 \cdot \ln x + 0.294$	0.647
(20)	$n_n + v_f$	not found	—	$c = -0.696 \cdot \ln x - 0.942$	0.885
(21)	$(1 - v_m) + v_f$	not found	—	$c = -0.647 \cdot \ln x - 0.647$	0.667
(22)	$n + (1 - v_m)$	$b = 0.650 \cdot \ln x + 0.657$[b]	0.681	$c = -0.666 \cdot \ln x - 0.996$[b]	0.932
(23)	$n + v_f$	not found	—	$c = -0.666 \cdot \ln x - 0.996$	0.933
Eq.	$\boldsymbol{p_1 + p_2}$	$\boldsymbol{b = f(x); x = \varepsilon_{m,Fmax} \cdot \delta}$	$\boldsymbol{R^2}$	$\boldsymbol{c = f(x); x = \varepsilon_{m,Fmax} \cdot \delta}$	$\boldsymbol{R^2}$
(18)	$n_{fp} + n_n$	$b = -0.525 \cdot \ln x - 0.815$	0.928	$c = 0.297 \cdot \ln x + 0.207$	0.714
(19)	$(1 - v_m) + n_n$	$b = -0.441 \cdot \ln x - 0.706$	0.903	$c = 0.262 \cdot \ln x + 0.182$	0.765
(20)	$n_n + v_f$	$b = 0.072 \cdot \ln x - 0.294$[a]	0.446	$c = -0.447 \cdot \ln x - 0.712$	0.931
(21)	$(1 - v_m) + v_f$	$b = 0.104 \cdot \ln x - 0.478$[a]	0.514	$c = -0.448 \cdot \ln x - 0.444$	0.793
(22)	$n + (1 - v_m)$	$b = 0.450 \cdot \ln x + 0.452$[b]	0.809	$c = -0.425 \cdot \ln x - 0.786$[b]	0.939
(23)	$n + v_f$	$b = 0.102 \cdot \ln x - 0.470$[a]	0.550	$c = -0.424 \cdot \ln x - 0.786$	0.936
Eq.	$\boldsymbol{p_1 + p_2}$	$\boldsymbol{b = f(x); x = \delta}$	$\boldsymbol{R^2}$	$\boldsymbol{c = f(x); x = \delta}$	$\boldsymbol{R^2}$
(18)	$n_{fp} + n_n$	$b = -1.050 \cdot \ln x - 0.431$	0.758	$c = 0.671 \cdot \ln x - 0.034$	0.741
(19)	$(1 - v_m) + n_n$	$b = -0.900 \cdot \ln x - 0.440$	0.657	$c = 0.604 \cdot \ln x + 0.003$	0.713
(20)	$n_n + v_f$	$b = -0.197 \cdot \ln x - 0.356$[a]	0.711	$c = -0.902 \cdot \ln x - 0.406$	0.730
(21)	$(1 - v_m) + v_f$	$b = 0.270 \cdot \ln x - 0.557$[a]	0.770	$c = -0.970 \cdot \ln x - 0.137$	0.717
(22)	$n + (1 - v_m)$	$b = 0.973 \cdot \ln x + 0.142$[b]	0.730	$c = -0.805 \cdot \ln x - 0.529$[b]	0.652
(23)	$n + v_f$	$b = 0.264 \cdot \ln x - 0.547$[a]	0.805	$c = -0.805 \cdot \ln x - 0.529$	0.652

[a]Excision of two devious points belonging to composites based on P_{33}-CO_{17}-Fe_{50} and P_{49}-CO_{26}-LO_{25} matrices.
[b]Dependencies depicted in Figure 6.

There are different versions of Equation (40) in the case of σ_{Fmax} without any significant advantage in the case of one of them against the second.

$$b = d + e \cdot \ln \sigma_{m,Fmax} \tag{43}$$

$$b = d + e \cdot \ln\left(\sigma_{m,Fmax} \cdot S_{m,rel}\right) \tag{44}$$

3.4 | Discussion With Comparison to Earlier Published Results

This work adds another insight to previous articles [32, 33] presenting Equations (1–3) that are possible to rewrite in one general form as:

$$z_c = z_m \cdot p_1^b \cdot p_2^c \tag{16}$$

And it introduces another equation shape ensuring the same phenomenon.

$$z_c = z_m + z_m \cdot \left(b \cdot p_1 + c \cdot p_2\right) \tag{17}$$

where p_1 and p_2 parameters have overturned values to Equation (16) and b and c members are numerically different.

It is impossible to avoid a comparison of Equations (16 and 17) from many perspectives in the discussion part. Although this work also describes relationships between structure/composition and mechanical properties of porous composites which means the same phenomenon as in the previous articles, by a little different means than in previous works, it is not a negation of the previous work [32, 33]. It is another point of view using little various means. Our opinion is that both equation shapes are interesting for further research. In this level of rough results, it is necessary to publish them both to be widely available to researchers. The decision of which shape is better is difficult. For instance, the fitting leads to different z_m values (z_m values from measurement were not available for comparison). It is impossible to decide now which result of the fitting is more appropriate in certain situations. The following research focused on composites based on nonporous matrices should answer for a direct comparison of fitted and measured z_m values. They could be inseparable and have to exist next to each other because their structural parameters are connected in mathematical relationships—see Equation (9). If is this valid, there is some basic idea connecting all equations in this work and those previous [32, 33]—presence of two suitable structural parameters and two describable fitting parameters in the equation. Although Equation (17) has one more member than Equation (16), the

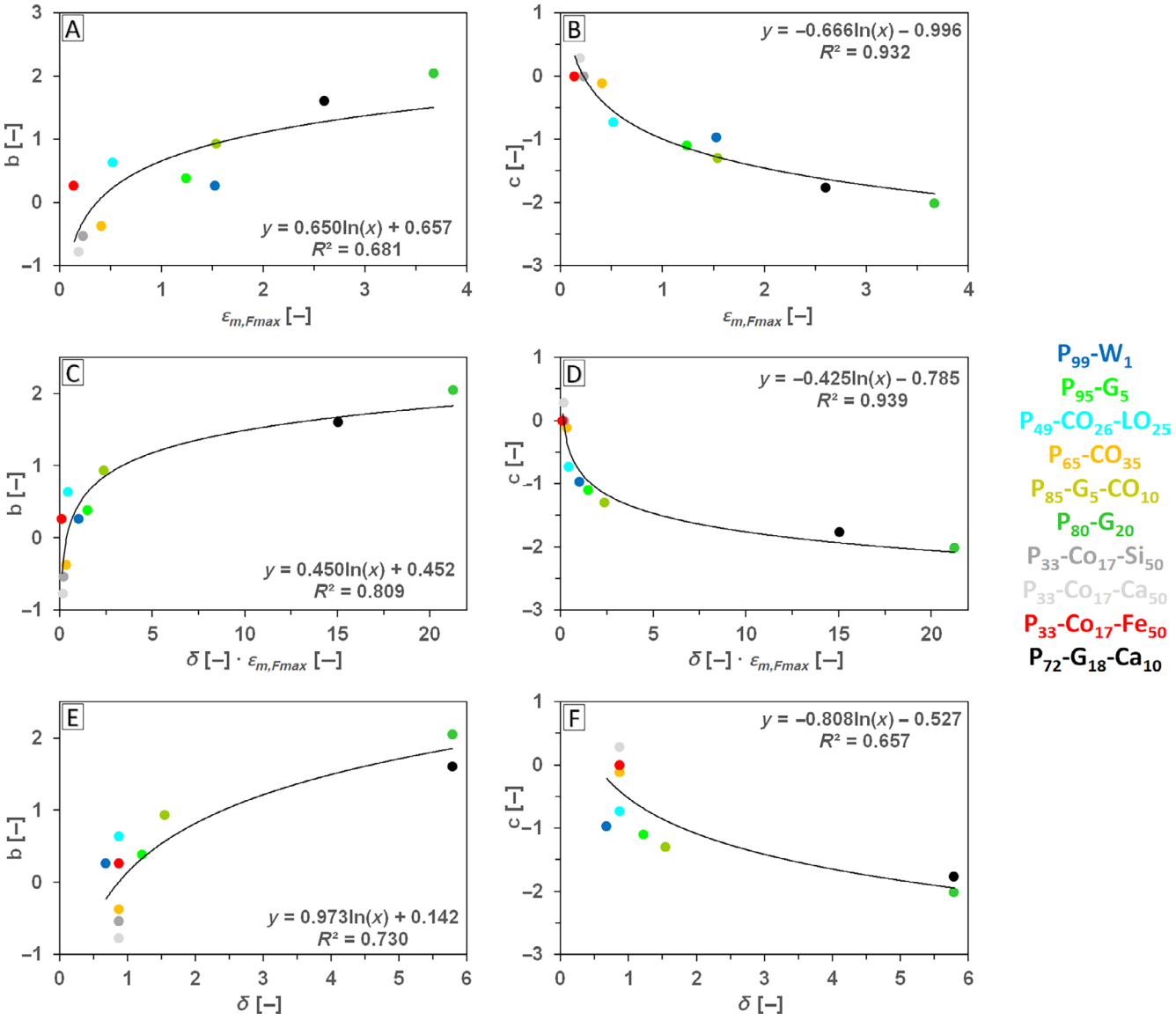

FIGURE 6 | Example of b (A, C, E) and c (B, D, F) parameters interpolations coming from fitting Equation (22) $z_c = z_m + z_m \cdot (b \cdot n + c \cdot (1 - v_m))$ derived for ultimate strain according to $\varepsilon_{m,Fmax}$ (A, B), $\varepsilon_{m,Fmax} \cdot \delta$ (C, D) and δ, (E, F), where $\varepsilon_{m,Fmax}$ values are from Table 5 and δ values from Table 1. [Color figure can be viewed at wileyonlinelibrary.com]

mathematical relationships are simpler in Equation (17) due to the absence of exponents and occurring mathematical sign types. The result of using the new structural parameters is the shape of Equation (17), which has to be linear if it is supposed to work correctly with the chosen structural parameters. However, they include more rich functions $b = f(c)$ in each fitted equation (see Table 7, not found in Equation (16)). Fitting leading to Equation (17) is not done only according to R^2 but also by the z_m fixation by the same value for slope and displacement. The interpolations are similar, with some variability, but the most common case is:

$$b = d + e \cdot \ln(z_m \cdot \delta); \quad c = f + g \cdot \ln(z_m \cdot \delta) \tag{45}$$

Equation (17) has three versions based on three structural parameters pairs created by three parameters (n, v_f, $1 - v_m$ instead of n_p, $1 - v_f$, and v_m from Equation (16)) and leading to the nearly same z_m values if they are compared (see Tables 3–6). The exact connection between the results from Equations (16 and 17) does not exist. The exception is only the Equation (9) dedicated to structural parameters. Further research should solve this problem after using nonporous matrices with the following direct comparison to measured and fitted values. There are also simple dependencies between b and c across different equations differing by structural parameters (n, v_f, $1 - v_m$ as example) in both relationships represented by Equations (17 and 16) (see Table 8 for Equation (17)). The possibility of simplified equations for nonporous composite (theoretically) and porous matrix (tested) is also valid for both approaches.

The primary data included materials with different matrices, various porosity rates (up to 50 vol% without the possibility of influence of its value during the preparation in a more

TABLE 12 | Interpolation possibilities of b and c parameters from Equations (18–23) with general shape $z_c = z_m + z_m \cdot (b \cdot p_1 + c \cdot p_2)$ for energy need for ultimate strength achievement according to $A_{m,Fmax}$, $A_{m,Fmax} \cdot \delta$, δ, $\varepsilon_{m,Fmax}$, $\varepsilon_{m,Fmax} \cdot \delta$ and $\sigma_{m,Fmax} \cdot \delta$, where $A_{m,Fmax}$ [kJ m^{-3}] values are from Table 6, $\varepsilon_{m,Fmax}$ [–] values are from Table 5, δ values from Table 1 and $\sigma_{m,Fmax}$ [MPa] values are from Table 4.

Eq.	$p_1 + p_2$	$b = f(x); x = A_{m,Fmax}$	R^2	$c = f(x); x = A_{m,Fmax}$	R^2
(18)	$n_{fp} + n_n$	$b = -0.750 \cdot \ln x + 3.558$	0.780	$c = 0.720 \cdot \ln x - 4.565$	0.769
(19)	$(1 - v_m) + n_n$	$b = -0.692 \cdot \ln x + 3.397$	0.708	$c = 0.723 \cdot \ln x - 4.662$	0.738
(20)	$n_n + v_f$	$b = 0.325 \cdot \ln x - 2.681$	0.772	$c = -0.643 \cdot \ln x + 3.052$	0.784
(21)	$(1 - v_m) + v_f$	$b = 0.477 \cdot \ln x - 4.027$	0.782	$c = -1.029 \cdot \ln x + 6.353$	0.840
(22)	$n + (1 - v_m)$	$b = 0.985 \cdot \ln x - 6.117$[a]	0.800	$c = -0.521 \cdot \ln x + 2.168$[a]	0.804
(23)	$n + v_f$	$b = 0.468 \cdot \ln x - 3.965$	0.778	$c = -0.525 \cdot \ln x + 2.186$	0.813
Eq.	$p_1 + p_2$	$b = f(x); x = A_{m,Fmax} \cdot \delta$	R^2	$c = f(x); x = A_{m,Fmax} \cdot \delta$	R^2
(18)	$n_{fp} + n_n$	$b = -0.538 \cdot \ln x + 2.448$	0.904	$c = 0.521 \cdot \ln x - 3.529$	0.907
(19)	$(1 - v_m) + n_n$	$b = -0.480 \cdot \ln x + 2.219$	0.683	$c = 0.505 \cdot \ln x - 3.457$	0.723
(20)	$n_n + v_f$	$b = 0.238 \cdot \ln x - 2.219$	0.887	$c = -0.457 \cdot \ln x + 2.057$	0.854
(21)	$(1 - v_m) + v_f$	$b = 0.351 \cdot \ln x - 3.351$	0.921	$c = -0.735 \cdot \ln x + 4.750$	0.931
(22)	$n + (1 - v_m)$	$b = 0.719 \cdot \ln x - 4.677$[a]	0.925	$c = -0.374 \cdot \ln x + 1.371$[a]	0.903
(23)	$n + v_f$	$b = 0.346 \cdot \ln x - 3.307$	0.920	$c = -0.376 \cdot \ln x + 1.370$	0.903
Eq.	$p_1 + p_2$	$b = f(x); x = \delta$	R^2	$c = f(x); x = \delta$	R^2
(18)	$n_{fp} + n_n$	$b = -1.257 \cdot \ln x - 0.578$	0.804	$c = 1.234 \cdot \ln x - 0.606$	0.830
(19)	$(1 - v_m) + n_n$	$b = -0.992 \cdot \ln x - 0.612$	0.398	$c = 1.064 \cdot \ln x - 0.486$	0.438
(20)	$n_n + v_f$	$b = 0.570 \cdot \ln x - 0.871$	0.777	$c = -1.045 \cdot \ln x - 0.553$	0.678
(21)	$(1 - v_m) + v_f$	$b = 0.806 \cdot \ln x - 1.300$	0.790	$c = -1.599 \cdot \ln x + 0.434$	0.719
(22)	$n + (1 - v_m)$	$b = 1.622 \cdot \ln x - 0.477$[a]	0.771	$c = -0.823 \cdot \ln x - 0.823$[a]	0.716
(23)	$n + v_f$	$b = 0.795 \cdot \ln x - 1.291$	0.796	$c = -0.823 \cdot \ln x - 0.823$	0.716
Eq.	$p_1 + p_2$	$b = f(x); x = \varepsilon_{m,Fmax}$	R^2	$c = f(x); x = \varepsilon_{m,Fmax}$	R^2
(18)	$n_{fp} + n_n$	$b = -0.836 \cdot \ln x - 1.318$	0.659	$c = 0.855 \cdot \ln x + 0.137$	0.738
(19)	$(1 - v_m) + n_n$	$b = -0.627 \cdot \ln x - 1.094$	0.380	$c = 0.687 \cdot \ln x + 0.036$	0.437
(20)	$n_n + v_f$	$b = 0.385 \cdot \ln x - 0.553$	0.723	$c = -0.667 \cdot \ln x - 1.121$	0.564
(21)	$(1 - v_m) + v_f$	$b = 0.546 \cdot \ln x - 0.873$	0.757	$c = -0.521 \cdot \ln x - 1.249$	0.599
(22)	$n + (1 - v_m)$	$b = 1.058 \cdot \ln x + 0.372$[b]	0.685	$c = -1.092 \cdot \ln x - 0.417$[b]	0.700
(23)	$n + v_f$	$b = -0.523 \cdot \ln x - 1.260$	0.596	$c = -0.523 \cdot \ln x - 1.260$	0.596
Eq.	$p_1 + p_2$	$b = f(x); x = \varepsilon_{m,Fmax} \cdot \delta$	R^2	$c = f(x); x = \varepsilon_{m,Fmax} \cdot \delta$	R^2
(18)	$n_{fp} + n_n$	$b = -0.572 \cdot \ln x - 1.031$	0.817	$c = 0.575 \cdot \ln x - 0.159$	0.883
(19)	$(1 - v_m) + n_n$	$b = -0.437 \cdot \ln x - 0.906$	0.440	$c = 0.475 \cdot \ln x - 0.170$	0.497
(20)	$n_n + v_f$	$b = 0.261 \cdot \ln x - 0.679$	0.846	$c = -0.463 \cdot \ln x - 0.903$	0.692
(21)	$(1 - v_m) + v_f$	$b = -0.376 \cdot \ln x + 1.044$	0.889	$c = -0.749 \cdot \ln x - 0.074$	0.817
(22)	$n + (1 - v_m)$	$b = 0.739 \cdot \ln x + 0.039$[b]	0.830	$c = -0.369 \cdot \ln x + 0.745$[b]	0.745
(23)	$n + v_f$	$b = -0370. \cdot \ln x - 1.038$	0.895	$c = -0.369 \cdot \ln x - 1.096$	0.737
Eq.	$p_1 + p_2$	$b = f(x); x = \sigma_{m,Fmax} \cdot \delta$	R^2	$c = f(x); x = \sigma_{m,Fmax} \cdot \delta$	R^2
(18)	$n_{fp} + n_n$	$b = -0.887 \cdot \ln x - 0.543$	0.765	$c = 0.806 \cdot \ln x - 0.609$	0.677

(Continues)

TABLE 12 | (Continued)

Eq.	p_1+p_2	$b=f(x); x=\sigma_{m,Fmax}\cdot\delta$	R^2	$c=f(x); x=\sigma_{m,Fmax}\cdot\delta$	R^2
(19)	$(1-v_m)+n_n$	$b=-0.887\cdot\ln x-0.414$	0.798	$c=0.900\cdot\ln x-0.669$	0.785
(20)	n_n+v_f	$b=0.362\cdot\ln x-0.878$	0.670	$c=-0.786\cdot\ln x-0.478$	0.823
(21)	$(1-v_m)+v_f$	$b=0.523\cdot\ln x-1.402$	0.669	$c=-1.172\cdot\ln x+0.726$	0.776
(22)	$n+(1-v_m)$	$b=1.137\cdot\ln x-0.736$[b]	0.760	$c=-0.630\cdot\ln x-0.656$[b]	0.841
(23)	$n+v_f$	$b=0.511\cdot\ln x-1.388$	0.660	$c=-0.634\cdot\ln x-0.664$	0.845

[a]Dependencies depicted in Figure 7.
[b]Dependencies depicted in Figure 8.

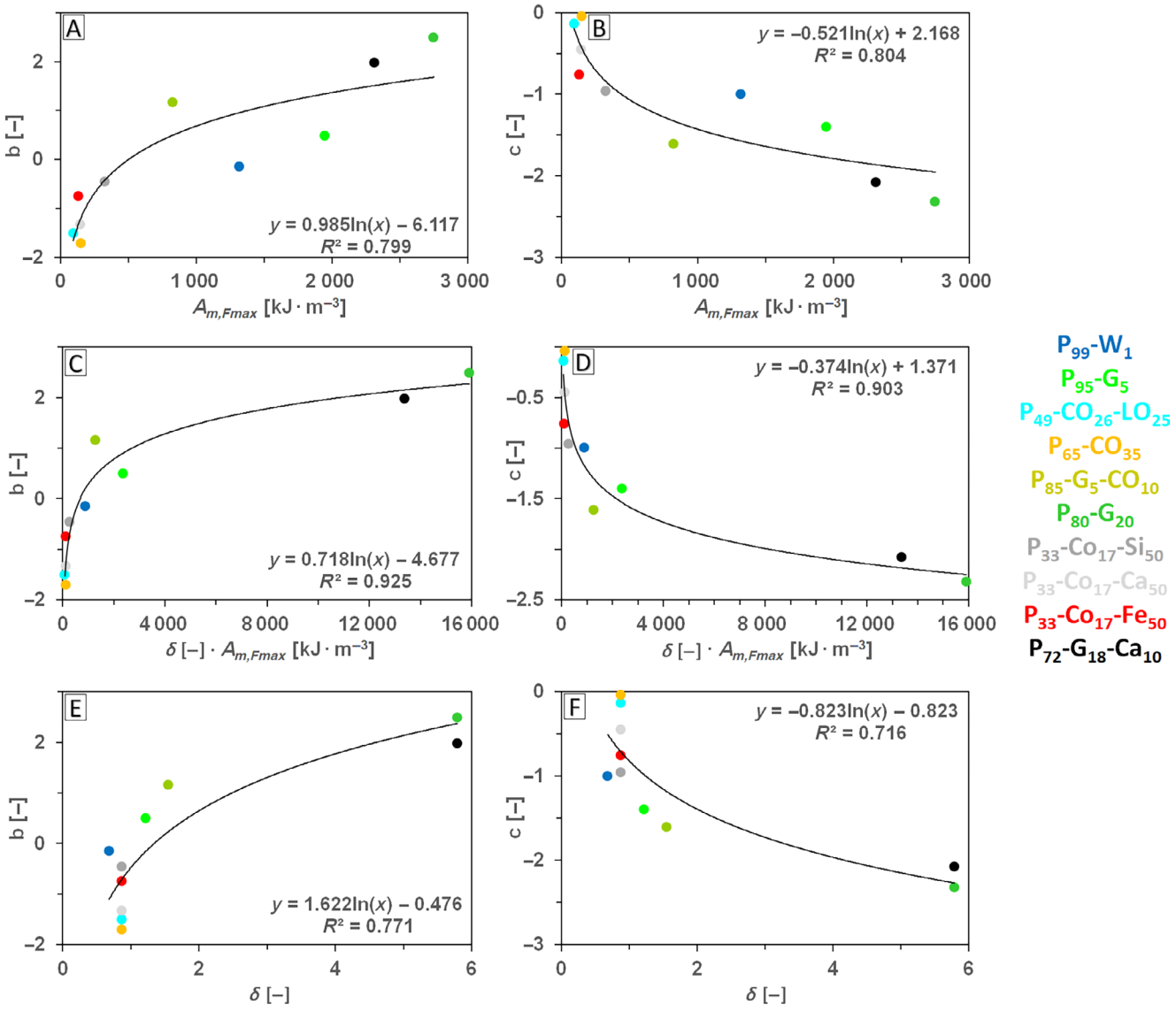

FIGURE 7 | Example of b (A, C, E) and c (B, D, F) parameters interpolations coming from fitting Equation (22) $z_c=z_m+z_m\cdot(b\cdot n+c\cdot(1-v_m))$ derived for energy need for ultimate strength achievement according to $A_{m,Fmax}$ (A, B), $A_{m,Fmax}\cdot\delta$ (C, D) and δ (E, F), where $A_{m,Fmax}$ values are from Table 6 and δ values from Table 1. [Color figure can be viewed at wileyonlinelibrary.com]

significant way), and only one type of filler (but including various filler contents). The filler behavior then cannot be accented in the shapes of relationships now. It could be included in the interpolation parameters d, e, f, and g with unclear behavior after research of composites based on different matrices but no fillers. Further research should focus on filler size distributions, surface values, surface properties, and their interaction with matrices. The surface properties of material

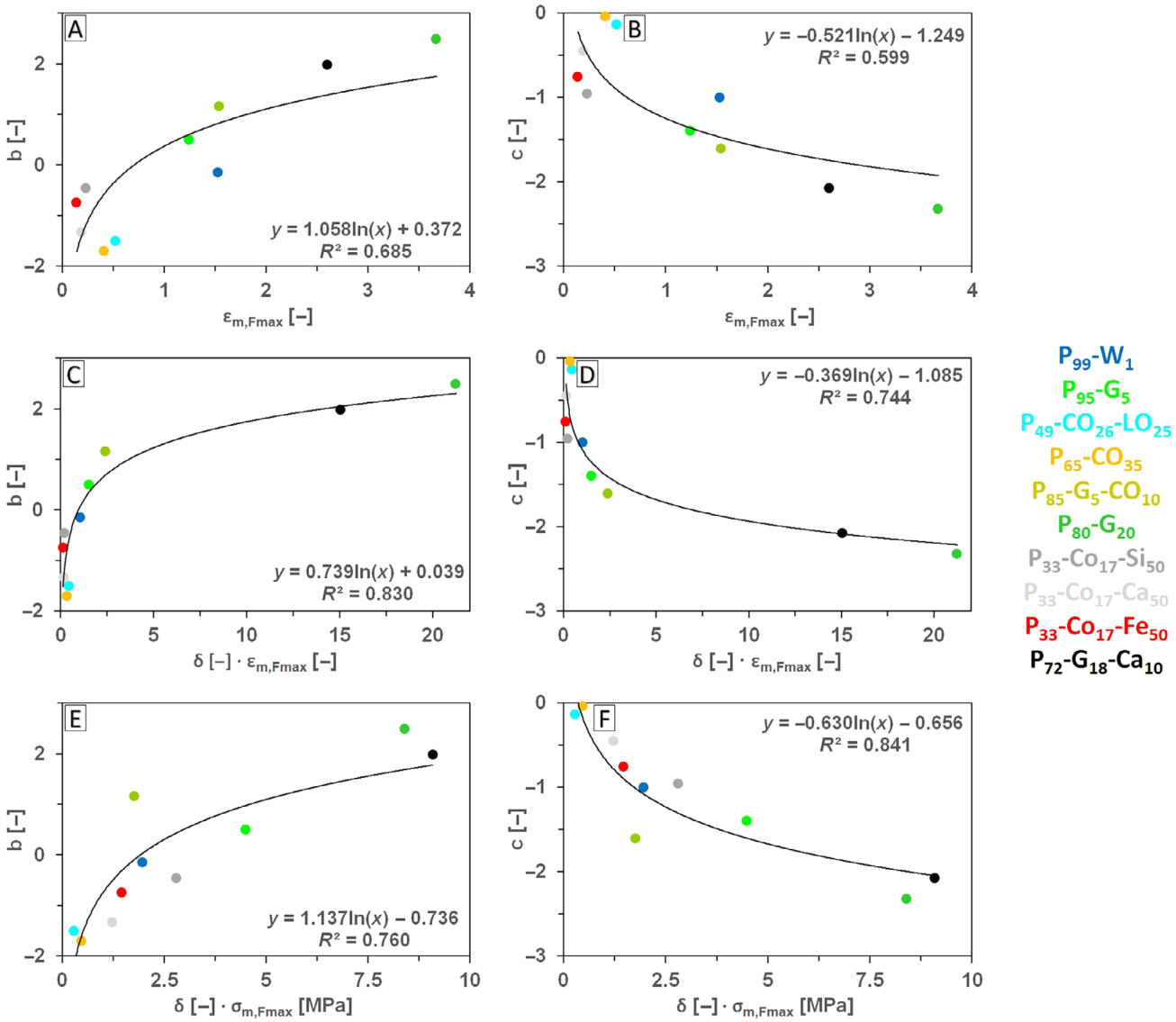

FIGURE 8 | Example of b (A, C, E) and c (B, D, F) parameters interpolations coming from fitting Equation (22) $z_c = z_m + z_m \cdot (b \cdot n + c \cdot (1 - v_m))$ derived for energy need for ultimate strength achievement according to $\varepsilon_{m,Fmax}$ (A, B), $\varepsilon_{m,Fmax} \cdot \delta$ (C, D), and $\sigma_{m,Fmax} \cdot \delta$ (E, F), where $\varepsilon_{m,Fmax}$ values are from Table 5, δ values from Table 1, and $\sigma_{m,Fmax}$ values are from Table 4. [Color figure can be viewed at wileyonlinelibrary.com]

components related to their adhesion should replace the δ value used as a simplification.

This work does not differ in the porosity type (open or closed pores) by visible means. There is an expectation that the porosity type (and its content in material) is a result of several factors such as matrix type, filler type, their rates, and ambient conditions affecting the porosity of the sample during its preparation—the pressing, for example. All these factors are directly or indirectly present in equation members, respectively, and their influence on them is expected (filler properties). There is also the question of the influence of void shapes and distribution to d and e parameters in simplified equations valid for porous matrices if the work focuses on the macroscopic point of view concerning the properties of components. Parameters d and e could be universal numbers for each one-component porous material, but it is necessary to prove it first. This work includes some effort to solve it. The limited data lead to only indication of results (low R^2), and this work should be repeated in another way in the future (more matrices with controlled porosity values for fitting, different shapes of voids if possible). Nevertheless, it is the first important step indicating future possibilities.

The proposed relationships for composites can process the data from materials on both sides of the percolation threshold in porosity/filler concentrations. It suggests an idea of utilization of similar equations in many different cases of not only the mechanical properties of materials.

The adjusted data processing approach could lead after discovering all relevant influences to relationships containing parameters adjustable according to types and rates of materials components. This approach could compose the composite behavior from the values of members in equations determined by the behavior of present components and their rates influenced by porosity if it would be present.

TABLE 13 | Interpolation possibilities of b parameters from Equation (40) with general shape $z_{mn}=z_m+z_m\cdot b\cdot n$ for elastic modulus/ultimate strength according to E_m and $E_m\cdot\delta/\sigma_{m,Fmax}$, and $\sigma_{m,Fmax}\cdot S_{m,rel}$, where E_m [MPa] values are from Table 3, $\sigma_{m,Fmax}$ [MPa] values are from Table 4, δ values from Table 1 and $S_{m,rel}$ from Equation (8).

Elastic modulus					
Eq.	$p_1+p_2\rightarrow p$	$b=f(x);x=E_m$	R^2	$b=f(x);x=E_m\cdot\delta$	R^2
(18)→(40)[a]	$n_{fp}+n_n\rightarrow n$	$b=-1.882\cdot\ln x+3.461$	0.533	Not found	—
(19)→(40)[a]	$(1-v_m)+n_n\rightarrow n$	$b=-11.24\cdot\ln x+24.14$	0.777	$b=-7.49\cdot\ln x+19.66$	0.562
(20)→(40)[a]	$n_n+v_f\rightarrow n$	$b=-5.68\cdot\ln x-11.68$	0.816	$b=-3.302\cdot\ln x+8.396$	0.458
(21)→(40)	$(1-v_m)+v_f\rightarrow n$	$b=2.861\cdot\ln x-8.887$	0.598	$b=2.566\cdot\ln x-8.937$	0.783
(22)→(40)	$n+(1-v_m)\rightarrow n$	$b=-3.179\cdot\ln x-9.579$[b]	0.586	$b=2.915\cdot\ln x-9.786$[b]	0.792
(23)→(40)	$n+v_f\rightarrow n$	$b=3.348\cdot\ln x-9.985$	0.600	$b=3.040\cdot\ln x-10.14$	0.795
Ultimate Strength					
Eq.	$p_1+p_2\rightarrow p$	$b=f(x);x=\sigma_{m,Fmax}$	R^2	$b=f(x);x=\sigma_{m,Fmax}\cdot S_{m,rel}$	R^2
(18)→(40)[a]	$n_{fp}+n_n\rightarrow n$	$b=-13.56\cdot\ln x+9.92$	0.664	$b=-14.69\cdot\ln x+0.26$	0.658
(19)→(40)[a]	$(1-v_m)+n_n\rightarrow n$	$b=-20.92\cdot\ln x+16.19$	0.739	$b=-24.95\cdot\ln x-0.41$	0.730
(20)→(40)[a]	$n_n+v_f\rightarrow n$	$b=-18.50\cdot\ln x-13.11$	0.727	$b=-21.25\cdot\ln x-0.71$	0.724
(21)→(40)[a]	$(1-v_m)+v_f\rightarrow n$	$b=-9.451\cdot\ln x+7.829$	0.701	$b=-11.56\cdot\ln x-0.16$	0.749
(22)→(40)[a]	$n+(1-v_m)\rightarrow n$	$b=-20.92\cdot\ln x+16.19$[b]	0.738	$b=-23.48\cdot\ln x-1.11$[b]	0.736
(23)→(40)[a]	$n+v_f\rightarrow n$	$b=-9.493\cdot\ln x-7.874$	0.706	$b=-11.63\cdot\ln x-0.13$	0.756

Note: Dependencies labeled by Equation (22)→(40) and parameters $n+(1-v_m)\rightarrow n$ are in Figure 9.
[a]Removal of a point belonging to the P_{65}-CO_{35} matrix due to its devious position, if needed.
[b]Dependencies depicted in Figure 9.

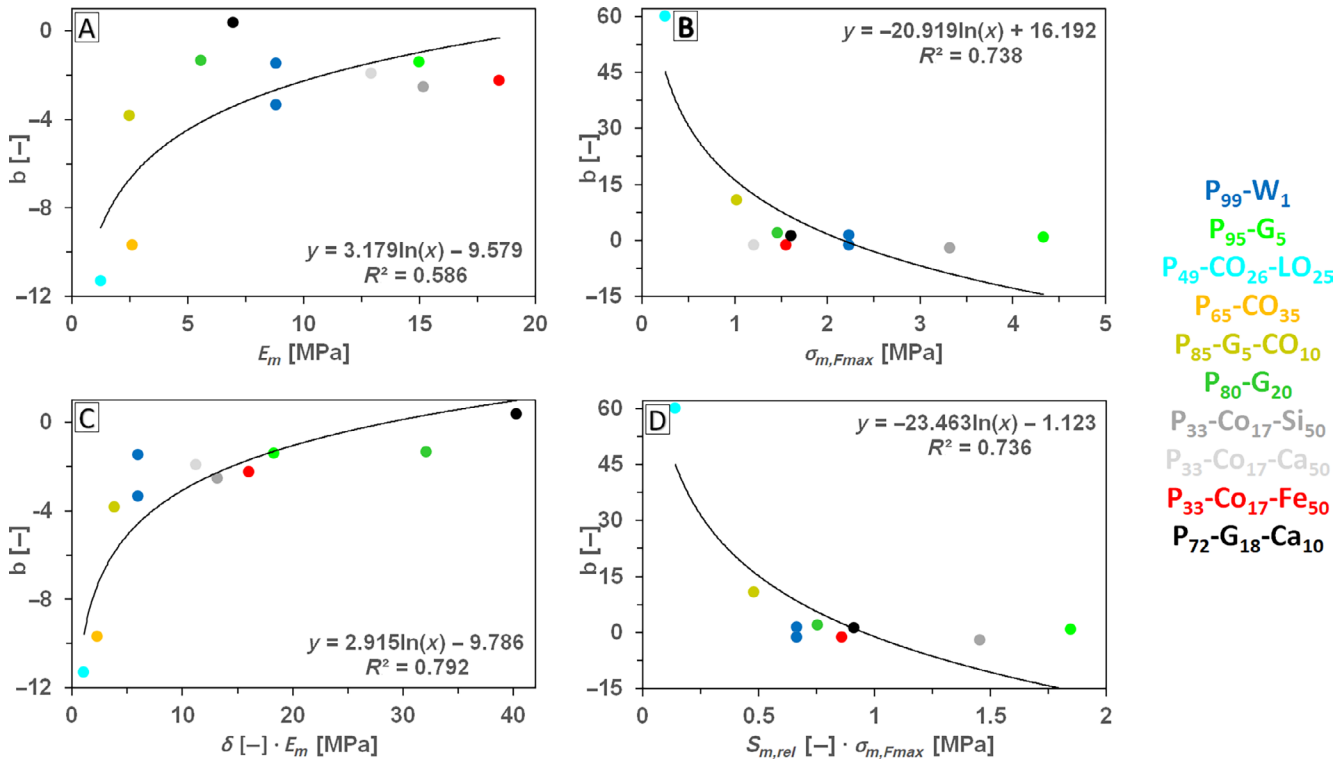

FIGURE 9 | Dependencies of b parameters values coming from Equation (40) $z_{mn}=z_m+z_m\cdot b\cdot n$ derived from Equation (22) valid for elastic modulus (A, C) and ultimate strength (B, D) on E_m (A), $E_m\cdot\delta$ (C), $\sigma_{m,Fmax}$ (B), and $\sigma_{m,Fmax}\cdot S_{m,rel}$ (D), where E_m values are from Table 3, $\sigma_{m,Fmax}$ values are from Table 4, δ values are from Table 1, and $S_{m,rel}$ values from Equation (8). [Color figure can be viewed at wileyonlinelibrary.com]

The base of our approach is relationships containing members determined accurately or approximately by their positions in equations and mathematical relations. First, materials with different compositions based on different matrices, fillers, and porosity can be prepared and tested. The work method is based on fitting measurement results to get an equation followed by equation members interpolation according to some properties and relations of components to find their mathematical behavior joined or comparable with the observed properties of components or the whole material.

It differs from most published works dedicated to physical models, where there is an accurate physical assumption at the beginning. This physical assumption is then compared with the behavior of existing material with some extent of accordance. The reason is simplification at the beginning—in material structure. In the model, it is hard to describe random structures containing randomly shaped particles and then randomly shaped pores. The expectations include granular particles [30], short fibers with cylindrical shapes [28], nanotubes or nanoparticles [23, 24] or unidirectionally oriented nanofibers [27] for example. Forms of voids can be limited to spherical [25]. The models are often limited to some properties. Examples include the elastic region of loading [21, 26–28] or the study of nonlinear stress [22–24, 29, 30]. The models can use different mathematical methods [21, 27–29].

The advantage of models is their awareness of physical rules, but there is often a problem with materials embodying random structures. Our proposed approach can work with randomly structured material due to its macroscopic point of view, and then it can describe also some stochastic properties, but not as well as elastic modulus. However, it does not work directly with an accurate physical description of the material on its microscopic level. Therefore, its understanding of phenomena occurring at a microscopic level is limited. It only connects the measured data with known properties of material components and structural parameters such as filler volume fraction, etc. These two approaches do not have to stand against each other. If our system were more complex (including also different filler types and maybe void types if it they are relevant), both approaches could meet in cases of material with a structure corresponding to limits of models such as spherical particles and voids, cylindrical particles, and so forth. This potential meeting or connection could contribute to understanding materials with different types of composition and structure complexity.

Our system of fitting and interpolating in presented forms comes from limited data set and needs continuation to solve a lot of question coming from proposed equations as filler and voids influence on material behavior.

4 | Conclusions

This work introduces new forms of description for relationships between structure/properties and chosen mechanical properties from tensile testing of porous materials (mainly filled composites, not reinforced). It uses the mean when the measurement is the beginning, the data fitting follows, and further interpolation of obtained parameters is the finish. The proposed relationships used structural parameters leading to a new shape of fitting functions (spatial linear with displacement). The fitting is newly based not only on the value of the R^2 coefficient but also on the similarity of slope and displacement values (they should be ideally the same) in the linear fitting function. The following interpolation gives real meaning to obtained parameters.

The proposed function shape is $z_c = z_m + z_m \cdot (b \cdot p_1 + c \cdot p_2)$, where z_c/z_m is generally labeled mechanical property value for composite/nonporous matrix, p_1/p_2 are suitable structural parameters, and b/c are fitting parameters subjected to interpolations by logarithmic function containing values of properties typical for matrices. The interpolations were done by as many means as possible to obtain many interpolation results. It serves as an indication of the potential research directions. The logarithmic functions interpolating the b and c parameters contain d, e, f, and g members without clear description. On the other hand, the work is not focused on different matrices and porosity types. Therefore, these interpolation members could be related to these material components and their behavior. The members p_1 and p_2 represent structural parameters including v_f (filer volume fraction), $1-v_m$ (volume fraction of filler and porosity together), n (porosity), n_{fp} (filler volume fraction, if porosity neglect), and n_n (interspace porosity) used in pairs. Combinations of the trinity of parameters—$1-v_m$, v_f, and n make the connection of proposed equations that include them. There is a connection of b and c parameters across equations and the retaining of slope and displacement values across different equations (if the property is the same). It is not valid for pairs p_1 and p_2 created by another combination of structural parameters. Another interesting result is the linear dependence of c on b in each proposed equation unconnected with the choice of structural parameters.

The proposed equations enable mathematical simplification if the corresponding material is simpler (without pores or filler) to only one structural parameter, one fitting parameter (b), and two interpolation parameters (d, e). The version valid for porous matrices was proven and the results were interesting but not sufficiently suitable due to the low amount of available data. The results are important because they indicate potential future research directions. The nonporous composites were not available and practically studied except for mathematically deriving their equation.

This work introduces new means of data processing that are non-exclusive to those earlier published and mentioned in this work as references or for comparisons. The results are rough, but they are shown in numerical forms (equations, values in tables) to enable easier looking for utilizable ways in further research. The most significant output of this work is the general shape of equations and mean of work (fitting, interpolation). The general output is more significant than individual results of fitting and interpolation, which are only its support.

Section 3 discusses the potential relationship of our work to physical models as another approach for investigating composite materials. Currently, there is no connection, but this could change in the future.

Author Contributions

Miroslav Černý: conceptualization (lead), data curation (equal), formal analysis (lead), investigation (lead), methodology (equal), writing – original draft (lead). **Přemysl Menčík:** conceptualization (supporting), data curation (equal), funding acquisition (lead), investigation (supporting), methodology (equal), writing – review and editing (lead).

Acknowledgments

This work was supported by the Brno University of Technology [Specific University Research Grant FCH-S-23-8208]. Open access publishing facilitated by Vysoke uceni technicke v Brne, as part of the Wiley - CzechELib agreement.

Conflicts of Interest

The authors declare no conflicts of interest.

Data Availability Statement

The data that support the findings of this study are available from the corresponding author upon reasonable request.

References

1. J. A. Choren, S. M. Heinrich, and M. B. Silver-Thorn, "Young's Modulus and Volume Porosity Relationships for Additive Manufacturing Applications," *Journal of Materials Science* 48 (2013): 5103–5112.

2. V. Krishna, S. Bose, and A. Bandyopadhyay, "Low Stiffness Porous Ti Structures for Load-Bearing Implants," *Acta Biomaterialia* 3 (2007): 997–1006.

3. A. P. Rubshtein, I. S. Trakhtenberg, E. B. Makarova, et al., "Porous Material Based on Spongy Titanium Granules: Structure, Mechanical Properties, and Osseointegration," *Materials Science and Engineering: C* 35 (2014): 363–369.

4. J. Kovacik, "Correlation between shear modulus and porosity in porous materials," *Journal of Materials Science Letters* 20 (2001): 1953–1955.

5. C. Lian, Y. Zhuge, and S. Beecham, "The Relationship Between Porosity and Strength for Porous Concrete," *Construction and Building Materials* 25 (2011): 4294–4298.

6. X. Fan, E. D. Case, F. Ren, Y. Shu, and M. J. Baumann, "Part II: Fracture Strength and Elastic Modulus as a Function of Porosity for Hydroxyapatite and Other Brittle Materials," *Journal of Mechanical Behavior of Biomedical Materials* 8 (2012): 99–110.

7. S. Karthikeyan, V. Balasubramanian, and R. Rajendran, "Developing Empirical Relationships to Estimate Porosity and Young's Modulus of Plasma Sprayed YSZ Coatings," *Applied Surface Science* 296 (2014): 31–46.

8. J. Kovacik, "Correlation Between Young's Modulus and Porosity in Porous Materials," *Journal of Materials Science Letters* 18 (1999): 1007–1010.

9. J. Kovacik, "Correlation Between Elastic Modulus, Shear Modulus, Poisson's Ratio and Porosity in Porous Materials," *Advanced Engineering Materials* 10 (2008): 250–252.

10. L. Y. Smolin, M. O. Eremin, M. P. Makarov, E. P. Evtushenko, S. N. Kulkov, and S. P. Buyakova, *AIP Conference Proceedings*, vol. 1 (Tomsk, Russia: AIP Publishing, 2014) Ch. 1623.

11. J. Werner, C. G. Aneziris, and S. Schaffoner, "Influence of Porosity on Young's Modulus of Carbon-Bonded Alumina From Room Temperature up to 1450°C," *Ceramics International* 40 (2014): 14439–14445.

12. L. Zhang, K. W. Gao, A. Elias, Z. G. Dong, and W. X. Chen, "Porosity Dependence of Elastic Modulus of Porous Cr3C2 Ceramics," *Ceramics International* 40 (2014): 191–198.

13. S. B. Sapozhnikov, O. A. Kudryavtsev, and N. Y. Dolganina, "Experimental and Numerical Estimation of Strength and Fragmentation of Different Porosity Alumina Ceramics," *Materials and Design* 88 (2015): 1042–1048.

14. Z. Wu, L. C. Sun, and J. Y. Wang, "Synthesis and Characterization of Porous Y 2 SiO 5 With Low Linear Shrinkage, High Porosity and High Strength," *Ceramics International* 42 (2016): 14894–14902.

15. M. F. Sonnenschein, "Porosity-Dependent Young's Modulus of Membranes From Polyetherether Ketone," *Journal of Polymer Science Part B: Polymer Physics* 41 (2003): 1168–1174.

16. V. Palchik, "Influence of Porosity and Elastic Modulus on Uniaxial Compressive Strength in Soft Brittle Porous Sandstones," *Rock Mechanics and Rock Engineering* 32 (1999): 303–309.

17. L. J. Gibson, M. F. Ashby, and K. E. Easterling, "Structure and Mechanics of the Iris Leaf," *Journal of Materials Science* 23 (1988): 3041–3048.

18. L. F. Nielsen, "Elasticity and Damping of Porous Materials and Impregnated Materials," *Journal of the American Ceramic Society* 67 (1984): 93–98.

19. X. Huiru and S. Quizhen, "Deformation Mechanisms and Mechanical Properties of Porous Magnesium/Carbon Nanofiber Composites With Different Porosities," *Journal of Materials Science* 53 (2018): 14375.

20. H. A. Bruck and B. H. Rabin, "Evaluating Microstructural and Damage Effects in Rule-of-Mixtures Predictions of the Mechanical Properties of Ni-Al_2O_3 Composites," *Journal of Materials Science* 34 (1999): 2241–2251.

21. X. J. Chao, W. L. Tian, F. Xu, and D. H. Shou, "A Fractal Model of Effective Mechanical Properties of Porous Composites," *Composites Science and Technology* 213 (2021): 108957.

22. N. Katsube and Y. N. Wu, "A Constitutive Theory for Porous Composite Materials," *International Journal of Solids and Structures* 35 (1998): 4587–4596.

23. H. Xu and Q. Li, "Effect of Carbon Nanofiber Concentration on Mechanical Properties of Porous Magnesium Composites: Experimental and Theoretical Analysis," *Materials Science and Engineering* 706 (2017): 249–255.

24. J. O. Odhiambo, M. Yoshida, A. Otsu, L.-F. Yi, T. Onda, and Z.-C. Chen, "Microstructure and tensile properties of in-situ synthesized and hot-extruded aluminum-matrix composites reinforced with hybrid submicron-sized ceramic particles," *Journal of Composite Materials* 56 (2022): 1987–2001.

25. L. Poh, C. Della, S. Ying, C. Goh, and Y. Li, "Micromechanics Model for Predicting Effective Elastic Moduli of Porous Ceramic Matrices With Randomly Oriented Carbon Nanotube Reinforcements," *AIP Advances* 5 (2015): 097153.

26. P. Alam, "A mixtures' model for porous particle–polymer composites," *Mechanics Research Communications* 37 (2010): 389–393.

27. A. T. Tran, H. Le Quang, and Q.-C. He, "Computation of the Size-Dependent Elastic Moduli of Nano-Fibrous and Nano-Porous Composites by FFT," *Composites Science and Technology* 135 (2016): 159–171.

28. H. K. Choi, M. J. Son, E. S. Shin, and J. Yu, "Prediction of Thermo-Poro-Elastic Properties of Porous Composites Using an Expanded Unmixing-Mixing Model," *Composite Structures* 188 (2018): 387–393.

29. C. Chan and H. E. Naguib, "Development and Characterization of Polypyrrole-Polylactide Conductive Open-Porous Composites," *Journal of Applied Polymer Science* 117 (2010): 3187–3195.

30. L. P. Khoroshun and E. N. Shikula, "Nonlinear Straining of Porous Composite Materials," *International Applied Mechanics* 29 (1993): 983–988.

31. Ö. Keleş, E. H. Anderson, J. Huynh, J. Gelb, J. Freund, and A. Karakoç, "Stochastic Fracture of Additively Manufactured Porous Composites," *Scientific Reports* 8 (2018): 15437.

32. M. Cerny, J. Petrus, and I. Chamradova, "The Influence of Porosity on Mechanical Properties of PUR-Based Composites: Experimentally Derived Mathematical Approach," *Polymers* 15 (2023): 1960.

33. M. Cerny, J. Petrus, F. Kucera, et al., "A New Approach to the Structure–Properties Relationship Evaluation for Porous Polymer Composites," *SN Applied Sciences* 2 (2020): 640.

34. A. S. Wagh, R. B. Poeppel, and J. P. Singh, "Open Pore Description of Mechanical Properties of Ceramics," *Journal of Materials Science* 26 (1991): 3862–3868.

35. Y. Chen and Y. F. Xu, "Compressive Strength of Fractal-Textured Foamed Concrete," *Fractals* 27 (2019): 1940003.

36. J. Teng, B. Yang, L.-Q. Zhang, et al., "Ultra-High Mechanical Properties of Porous Composites Based on Regenerated Cellulose and Cross-Linked Poly(Ethylene Glycol)," *Carbohydrate Polymers* 179 (2018): 244–251.

37. S. Węgrzyk and D. Herman, "Strengthening of Al_2O_3 Porous Composites With a Glass-Ceramic Binder Doped With Nanocopper," *Journal of the European Ceramic Society* 41 (2021): 5558–5569.

38. L. Olmos, A. S. Gonzalés-Pedraza, H. J. Vergara-Hernández, et al., "Ti64/20Ag Porous Composites Fabricated by Powder Metallurgy for Biomedical Applications," *Materials* 15 (2022): 5956.

39. J. Seuba, E. Maire, J. Adrien, S. Meille, and S. Deville, "Mechanical Properties of Unidirectional, Porous Polymer/Ceramic Composites for Biomedical Applications," *Open Ceramics* 8 (2021): 100195.

40. M. Krzesinska, "Influence of the Raw Material on the Pore Structure and Elastic Properties of Compressed Expanded Graphite Blocks," *Materials Chemistry and Physics* 87 (2004): 336–344.

41. K. K. Phani and R. N. Mukerjee, "Elastic Properties of Porous Thermosetting Polymers," *Journal of Materials Science* 22 (1987): 3453–3458.

42. K. K. Phani and S. K. Niyogi, "Elastic Modulus-Porosity Relationship for Si3N4," *Journal of Materials Science Letters* 6 (1987): 511–515.

43. K. K. Phani and S. K. Niyogi, "Young's Modulus of Porous Brittle Solids," *Journal of Materials Science* 22 (1987): 257–263.

Supporting Information

Additional supporting information can be found online in the Supporting Information section.